Numerička analiza učinkovitosti HULA brtve

Wolff, Daniel

Master's thesis / Diplomski rad

2017

Degree Grantor / Ustanova koja je dodijelila akademski / stručni stupanj: **University of Zagreb, Faculty of Mechanical Engineering and Naval Architecture / Sveučilište u Zagrebu, Fakultet strojarstva i brodogradnje**

Permanent link / Trajna poveznica: https://urn.nsk.hr/urn:nbn:hr:235:731727

Rights / Prava: In copyright/Zaštićeno autorskim pravom.

Download date / Datum preuzimanja: **2024-12-24**

UNIVERSITY OF ZAGREB
FACULTY OF MECHANICAL ENGINEERING AND NAVAL
ARCHITECTURE

MASTER'S THESIS

Daniel Wolff

Zagreb, 2017.

UNIVERSITY OF ZAGREB
FACULTY OF MECHANICAL ENGINEERING AND NAVAL
ARCHITECTURE

NUMERICAL ANALYSIS OF HULA SEAL PRFORMANCE

Supervisor: Student:

Assoc. Prof. dr. sc. Željko Tuković   Daniel Wolff

Zagreb, 2017.

Sveučilište u Zagrebu	
Fakultet strojarstva i brodogradnje	
Datum	Prilog
Klasa:	
Ur.broj:	

DIPLOMSKI ZADATAK

Student: Daniel Wolff   Mat. br.: 0035180204

Naslov rada na
hrvatskom jeziku: **Numerička analiza učinkovitosti HULA brtve**

Naslov rada na
engleskom jeziku: **Numerical analysis of HULA seal performance**

Opis zadatka:

Many years of progress and evolution brought heavy duty gas turbine engines, equipped with silo combustion chambers to a high level of performance and reliability. Rising demands on emission reduction set a task to minimize the amount of cooling and leakage air, without negative impact on the lifetime of the components. Silo combustion chambers are characterised by the large-scale cylindrical interfaces between the hot gas path components. During the gas turbine operation, the creep deformations of the interfaces can occur and proper sealing becomes a very challenging task.

Annular flexible spring finger seals, also known as HULA seals, are used to compensate misalignment between co-annular parts, while providing effective sealing performance. Hula seals are circumferential metal seals that are slotted in the axial direction and contoured to be spring-loaded between inner and outer diameters of the matching parts that experience relative axial motion. Long term successful implementation of the HULA seals for sealing of stationary interfaces for industrial and aero gas turbine engines confirmed benefits from the application as are: improved lifetime of the hot gas parts, reduction of manufacturing costs and on-site assembly time.

In the scope of this thesis, computational fluid dynamic method will be used to verify the sealing performance of the HULA seal with the application to the large-scale interfaces. Thermal conditions of the HULA seal as well as interfacing components will be studied with a target to define the optimum geometry fulfilling design requirements with the minimum air consumption. Upon the definition of the optimum HULA seal arrangement, an off-design sensitivity study of the potential contour shape deviations will be conducted.

It is advised to list references used in this work, as well as to acknowledge help and support possibly received during the course of this study.

Zadatak zadan: Rok predaje rada: Predviđeni datumi obrane:

17. studenog 2016.   19. siječnja 2017.   25., 26. i 27. siječnja 2017.

Zadatak zadao: Predsjednica Povjerenstva:

Izv.prof.dr.sc. Željko Tuković   Prof. dr. sc. Tanja Jurčević Lulić

Table of Contents

List of Figures

List of Tables

Nomenclature

Greek letters

α_p	$W/(m^2 \cdot K)$	Heat transfer coefficient
α_ω		Correction factor
$a^{u_k p}$		Coefficient derived from the Gauss divergence theorem
ε	m^2/s^3	Dissipation of turbulent kinetic energy
κ		Von Karman constant
θ_e		The angle for equiangular face or cell
θ_{max}		Largest angle in a face or cell
θ_{min}		Smallest angle in a face or cell
μ	$Pa \cdot s$	Dynamic viscosity
μ_T	$Pa \cdot s$	Turbulent viscosity
ν	m^2/s^2	Kinematic viscosity
ρ	kg/m^2	Density
τ	N/m^2	Tangential stress
τ_ω	N/m^2	Tangential stress in viscous sub-layer
$\emptyset$		Variable in center of control volume
$\overline{\emptyset_f}$		Variable in center of control surface
$\overline{\emptyset_n}$		Variable in node of control volume
ω	m^2/s^2	Specific turbulence dissipation

Latin letters

A_f	m^2	Size of control surface
C		Coefficient
C		Integration constant
C_p	$J/(kgK)$	Heat capacity at constant pressure
F	N	Force
k	m^2/s^2	Turbulent kinetic energy
k	$W/(mK)$	Thermal conductivity
n		Normal vector
N_f		Number of nodes
p	Pa	Static pressure

q	W/m	Heat flux
Q	W	Heat transfer
u	m/s	Velocity
u^+		Dimensionless velocity
u_*		Friction velocity at the nearest wall
V	m^3	Element volume
R	J/(kgK)	Gas constant
S	m^2	Surface
T	k	Temperature
t	s	Time
y	m	Distance to the nearest wall
y^+		Dimensionless distance form solid surface

SAŽETAK

(ABSTRACT IN CROATIAN)

NUMERIČKA ANALIZA UČINKOVITOSTI HULA BRTVE

Ovaj rad bavi se brtvljenjem velikih sučelja između gornjeg i donjeg dijela unutarnjeg kućišta komore izgaranja u silo izvedbi. Provedena je analiza učinkovitosti hlađenja hula brtve koja bi zamijenila staru belt brtvu. Hula brtva je fleksibilna prstenasta brtva koja se koristi za kompenzaciju pomaka između dvije cilindrične komponente, a da pritom pruža učinkovitu izvedbu brtvljenja. Plinska turbina na koju će se ugraditi hula brtva je starija plinska turbina s komorom izgaranja u silo izvedbi koja koristi belt brtvu za brtvljenje sučelja između gornjeg i donjeg dijela unutarnjeg kućišta komore izgaranja. Glavni razlog za odabir ove plinske turbine je veliko trošenje i troškovi popravka same belt brtve i sučelja između gornjeg i donjeg dijela unutarnjeg kućišta komore izgaranja u odnosu na druge slične plinske turbine.

U okviru ovoga rada računalna dinamika fluida korištena je za provjeru učinkovitosti hula brtve i uspoređena je sa učinkovitosti belt brtve. Za gornji i donji dio unutarnjeg kućišta komore izgaranja te za belt brtvu korišteni su već postojeći geometrijski modeli dok je model hula brtve izrađen prema patentu hula brtve. Iz tih modela sklopljena su dva slučaja, onaj sa belt brtvom i onaj sa hula brtvom. Za numeričku analizu korišten je periodički isječak iz cijele geometrije oba slučaja radi smanjenja vremena računanja. Numerička analiza uključuje volumen kroz koji struji fluid te stijenku unutarnjeg kućišta kako bi se ispitala interakcija između njih odnosno da bi se saznalo kako hlađenje zrakom utječe na toplinske uvijete komponenti. Dobiveni rezultati sadrže polja tlakova, brzina i temperatura, te strujnice kako bi se što bolje opisali toplinski uvjeti i strujanje fluida. Na temelju rezultata izveden je zaključak da hula brtva u odnosu na belt brtvu nije dovoljno učinkovita odnosno ne osigurava potrebno hlađenje kućišta komore izgaranja. Kao preporuka za povećanje učinkovitosti navedene su promjene na samoj hula brtvi.

Ključne riječi:

Hula brtva, numerička analiza, plinska turbina, komora izgaranja, prijelaz topline

PROŠIRENI SAŽETAK NA HRVATSKOM

(EXTENDED ABSTRACT IN CROATIAN)

1. Uvod

Stare plinske turbine koje su još uvijek u pogonu mogu se nadograditi novo razvijenim komponentama. Kada životni ciklus starih komponenti završi zamjenjuju se novim po mogućnosti boljim komponentama. Novo razvijene komponente jednako su kvalitetne ako ne i bolje od starih, te su često jeftinije za proizvodnju i jednostavnije za montažu. Dulji životni vijek je glavno svojstvo koje karakterizira nove komponente boljim od starih. Parametri koji će se uspoređivati su učinkovitost hlađenja i protok propuštanja zraka kroz brtve. Uspoređene su dvije brtve: trenutno standardna belt brtva i nova hula brtva. Stara belt brtva analizira se kako bi dobili bolji uvid u strukturu toka fluida i da bi usporedili učinkovitost s hula brtvom. Glavni razlog za numeričku analizu rada je analiza učinkovitosti hula brtve u plinskoj turbini koja trenutačno koristi staru belt brtvu. Kako bi lakše usporedili učinkovitost dviju brtvi rezultati numeričke analize sadržavati će polja temperatura, tlaka, brzina, iznose masenih protoka te trodimenzionalnu strukturu strujanja koja će se prikazati strujnicama. Na temelju rezultata numeričke simulacije dati će se usporedba i prijedlozi za poboljšanje učinkovitosti.

1.1. Plinska turbina s komorom izgaranja u silo izvedbi

U ovom odjeljku biti će prikazan princip rada plinske turbine sa komorom izgaranja u silo izvedbi. Zrak iz okoliša ulazi u kompresor gdje je komprimiran u nekoliko stupnjeva. Izlaskom iz kompresora struji između zida kućišta plinske turbine i izvan dijela unutarnjeg kućišta komore izgaranja. Tu se zrak predgrijava pritom hladeći donji dio unutarnjeg kućišta komore izgaranja, a zatim i gornji dio unutarnjeg kućišta komore izgaranja. Nakon prolaska tim kanalima izvan komore izgaranja gdje je predgrijan miješa se sa gorivom i ubacuju u komoru izgaranja. Vruća smjesa dimnih plinova i zraka nakon izgaranja putuje prema dolje unutar silo komore izgaranja odnosno unutar gornjeg dijela unutarnjeg kućišta komore izgaranja. Iz njega ulazi u donji dio unutarnjeg kućišta komore izgaranja gdje je ta smjesa vrućih plinova usmjerena prema turbini, gdje ekspandira, pogoni turbinu i proizvodi rad.
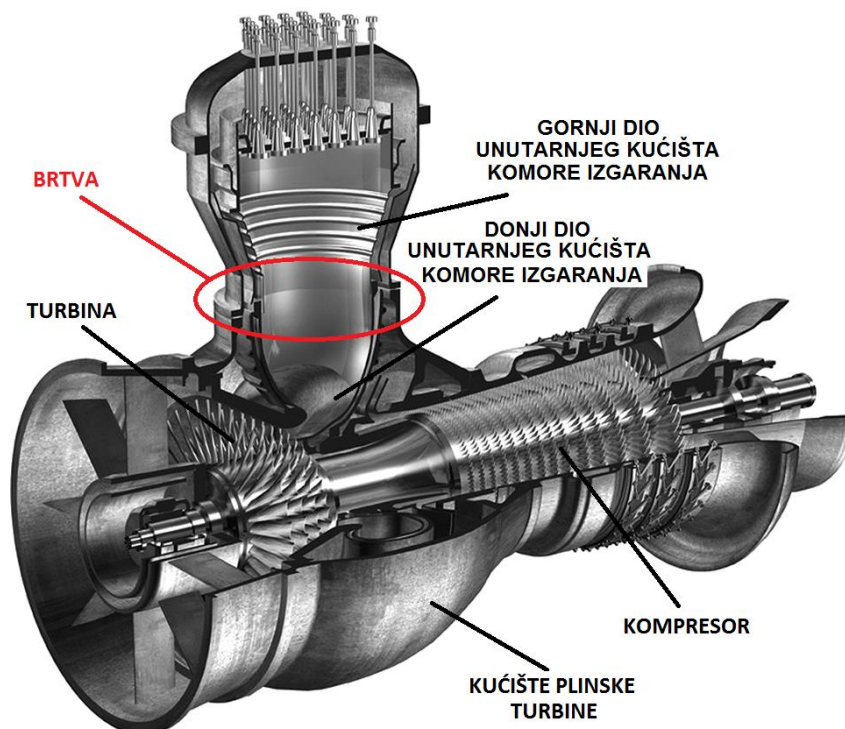
Slika 1. Plinska turbina sa komorom izgaranja u silo izvedbi

1.2. Gornji i donji dio unutarnjeg kućišta komore izgaranja

Glavni dijelovi plinske turbine su kompresor, komora izgaranja i turbina. Svi dijelovi plinske turbine zatvoreni su u samom kućištu. Glavni dio komore izgaranja je sam prostor u kojem se događa izgaranje koje je zatvoreno sa gornjim dijelom unutarnjeg kućišta i donjim dijelom unutarnjeg kućišta komore izgaranja. Tijekom rada plinska turbina izgaranjem proizvodi vruće dimne plinove unutar komore izgaranja. Komprimirani zrak iz kompresora struji prema komori izgaranja kroz prostor koji se nalazi između donjeg dijela unutarnjeg kućišta komore izgaranja i kućišta plinske turbine. Zbog toga što je komprimirani zrak niže temperature od površine donjeg dijela unutarnjeg kućišta komore izgaranja toplina sa stjenke prelazi na zrak. Zato kažemo da je donji dio unutarnjeg kućišta komore izgaranja hlađen komprimiranim zrakom. Nakon donjeg dijela unutarnjeg kućišta komore izgaranja komprimirani zrak struji izvan gornjeg dijela unutarnjeg kućišta komore izgaranja i pritom ga hladi. Na kraju takav predgrijan komprimirani zrak ulazi u komoru izgaranja. Unutarnje kućište komore izgaranja je dio komore izgaranja koji dijeli hladan zrak od vrućih plinova. U komori izgaranja gorivo se ubrizgava u struju zraka. Mješavina tih plinova izgara i generira toplinu. Vrući dimni plinovi zatim izlaze iz prostora u kojem izgara i ulaze u donji dio unutarnjeg kućišta komore izgaranja. Zbog vrlo visokih temperatura vrućih dimnih plinova u gornjem dijelu unutarnjeg

kućišta i donjem dijelu unutarnjeg kućišta komore izgaranja vrlo je važno da budu što bolje hlađeni zrakom. Vrući dimni plinovi iz gornjeg dijela unutarnjeg kućišta komore izgaranja ulaze u turbinu. Metodom kojom se hlade ovi dijelovi komore izgaranja dovode do neuniformnog strujanja komprimiranog zraka izvan gornjeg i donjeg dijela unutarnjeg kućišta komore izgaranja. Rezultat takvog strujanja odnosno hlađenja su neuniformnog temperature stjenke gornjeg i donjeg dijela unutarnjeg kućišta komore izgaranja koje dovode do termalnih naprezanja u samom materijalu. Takva naprezanja mogu dovesti do pukotina odnosno smanjivanja životnog vijeka samih komponenti.
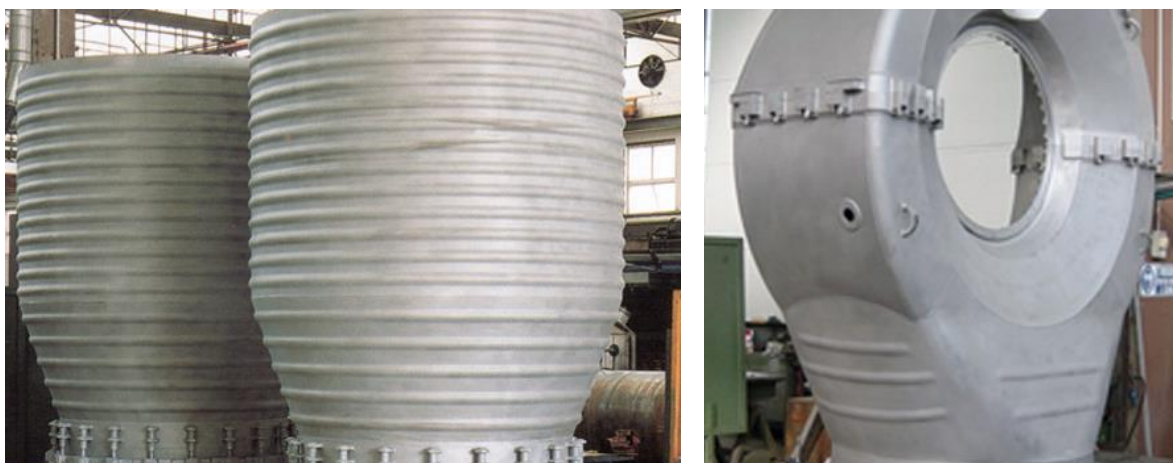
Slika 2. Gornji i donji dio unutarnjeg kućišta komore izgaranja

1.3. Brtva između gornjeg i donjeg dijela unutarnjeg kućišta komore izgaranja

U starim plinskim turbinama gornji i donji dio unutarnjeg kućišta komore izgaranja instalirani su s preklapanjem bez brtve između ta dva dijela. Krajem 1970-tih razvijena je brtva koja se sastojala od segmenata. Ta brtva koristi se još i danas na nekim starim plinskim turbinama. Propuštanje kroz procijep u segmentima generiralo je lokalno pregaranje na dijelovima gornjeg i donjeg dijela unutarnjeg kućišta komore izgaranja. Ovaj efekt brzo se uočio zbog čestih pucanja i smanjivanja životnog vijeka ovih dijelova turbine. Zbog toga se krenulo u razvoj nove brtve, belt brtve u nekoliko koraka. Od 1990-tih belt brtva je standardni dio plinskih turbina sa komorom izgaranja u silo izvedbi. Belt brtva poboljšala je učinkovitost hlađenja u odnosu na prethodnu brtvu, međutim na pojedinim plinskim turbinama i dalje se javlja isti efekt koji dovodi do pucanja i smanjenja životnog vijeka komponenti. Ovaj problem pokušavao se riješiti analizama i poboljšanjima same belt brtve. Razne modifikacije dizajna same brtve su naprevljene međutim problem nikad nije do kraja riješen.
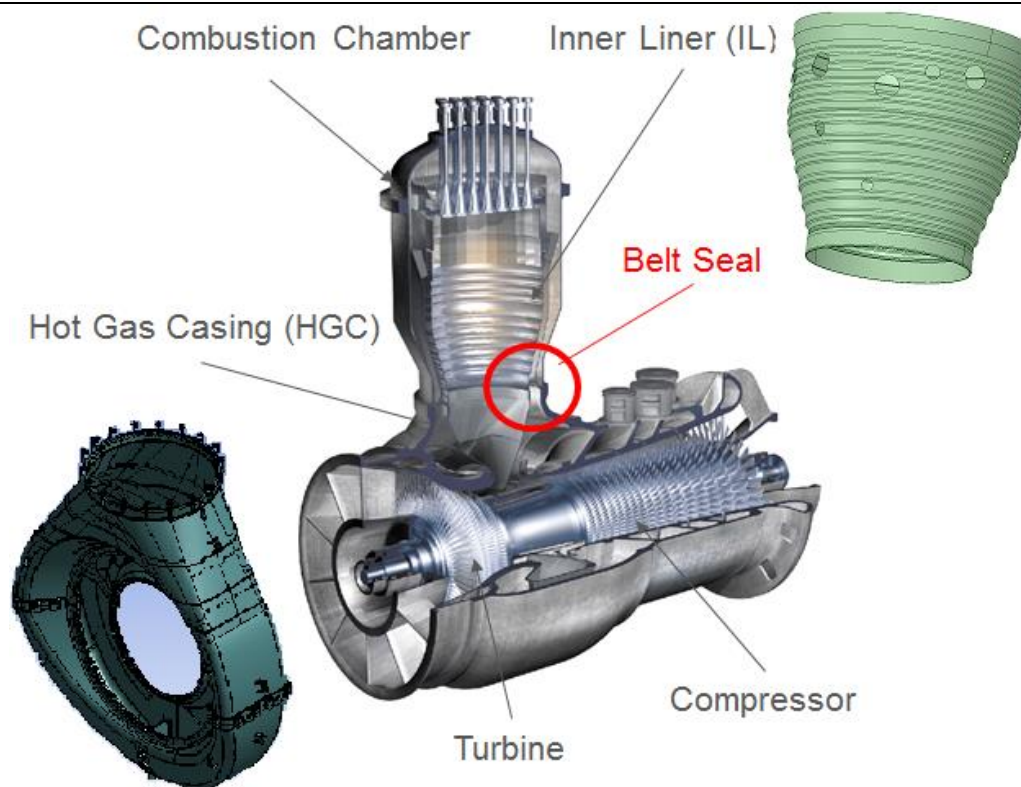
Slika 3. Mjesto u plinskoj turbini na koje se ugrađuje belt brtva

Danas se standardna belt brtva za plinske turbine sa komorom izgaranja u silo izvedbi želi zamijeniti sa novijom hula brtvom. Neki proizvođači plinskih turbina imaju dugogodišnje iskustvo uspješnog korištenja hula brtve. Očekivane koristi od primjene nove hula brtve na starim plinskim turbinama su: produženje vijeka trajanja komponenti komore izgaranja, smanjenje troškova proizvodnje i skraćivanje vremena montaže.

1.4. Belt brtva

Belt brtva vrsta je brtve korištena između dvije komponente komore izgaranja u plinskim turbinama, između gornjeg i donjeg dijela unutarnjeg kućišta komore izgaranja. Sastoji se od segmenata koji su međusobno povezani oprugama. Broj segmenata belt brtve ovisi o veličini samog segmenta odnosno o veličini sučelja između gornjeg i donjeg dijela unutarnjeg kućišta komore izgaranja. Belt brtva korištena u ovome radu sastoji se od 18 segmenata te je promjer sučelja 1,4 m. Ova brtva smanjuje propuštanje zraka za hlađenje koji prolazi kroz nju ne smanjujući učinkovitost hlađenja. Određeni dio propuštanja zraka kroz prolaze na belt brtvi je nužan kako bi se osiguralo hlađenje same brtve i unutarnji dio komponenti koje sačinjavaju sučelje. Kako je i gore navedeno, belt brtva razvijena u nekoliko koraka i od 1990-tih godina

standardna je kod plinskih turbina sa komorom izgaranja u silo izvedbi. Glavni problem ove brtve je fenomen lokalnog pregaranja unutrašnjih dijelova gornjeg i donjeg dijela unutarnjeg kućišta komore izgaranja. Glavni izazov danas je povećati učinkovitost hlađenja, produžiti životni vijek ovih komponenata, reducirat cijenu izrade same brtve i smanjiti vrijeme montaže brtve.

Slika 4. Jedan segment belt brtve i ugrađena belt brtva na donji dio unutarnjeg kućišta komore izgaranja

1.5. Hula brtva

Nekoliko tvrtki koje proizvode plinske turbine koriste hula brtvu za brtvljenje sučelja između gornjeg i donjeg dijela unutarnjeg kućišta komore izgaranja. Slične hula brtve mogu se koristiti za brtvljenje između drugih sličnih dijelova plinske turbine. U ovome radu standardna belt brtva biti će zamijenjena sa novom hula brtvom. Kao što je navedeno u patentu U.S. Pat. No. 6,334,310, hula brtva je generalno definirana kao sustav lisnate opruge formirane u kružni oblik i koji se koristi za brtvljenje prstenastih raspora između dva koncentrična kanala. Određeni protok zraka kroz hula brtvu se propušta kako bi hladila samu sebe ali i komponente koje čine sučelje, za naš slučaj to su: gornji i donji dio unutarnjeg kućišta komore izgaranja. Održavanje niskih temperatura sučelja, odnosno dijelova sučelja glavni je zadatak hula brtve. Povećanje masenog protoka zraka kroz prolaze na brtvi poboljšalo bi hlađenje komponenti, međutim to nije moguće jer bi se poremetio dovod komprimiranog zraka u komoru izgaranja koji je potreba za samo izgaranje. Fokus ovog rada je usporedba hlađenja i utjecaj na maseni protok zraka radi zamjene belt brtve sa novom hula brtvom. Dizajn hula brtve može varirati odnosno on ovisi o geometriji samoga sučelja i potrebama za hlađenje. U našem slučaju najvažnije je hlađenje gornjeg i donjeg dijela

unutarnjeg kućišta komore izgaranja kao i same brtve kako bi se produžio životni vijek tih komponenti.

Slika 5. Hula brtva

1. Matematički model

Strujanje fluida opisano je Navier-Stokes jednadžbama. Analitičkog rješenja općeg oblika tih jednadžbi nema zbog njihove nelinearne prirode. Potrebno je uvoditi određene pretpostavke o strujanju fluida kako bi se one pojednostavile. Tako je neke generičke oblike strujanja moguće analitički proračunati. Danas je izgled i karakteristike nekog općenitog strujanja moguće dobiti samo eksperimentalnim ili numeričkim putem. Rješavanje problema numeričkim simulacijama izvodi se u nekoliko koraka:

- Odabir matematičkog modela
- Rješavanje matematičkog modela
    - Prostorna diskretizacija domene strujanja
    - Diskretizacija jednadžbi matematičkog modela
    - Rješavanje sustava algebarskih jednadžbi
- Analiza dobivenoga rješenja

Matematički model je sustav parcijalnih diferencijalnih jednadžbi kojima se opisuje fizikalni problem. Rješavanje matematičkog modela zahtjeva da se prostorna domena strujanja podijeli na manje dijelove, kontrolne volumene, u kojima se može pretpostaviti homogeno strujanje fluida. Rezultat te prostorne diskretizacije je geometrijska mreža na kojoj se diskretiziraju jednadžbe matematičkog modela. Diskretizacija jednadžbi vrši se pomoću neke od metoda (metoda konačnih volumena, metoda konačnih elemenata, metoda konačnih razlika, ...). U simulacijama dinamike fluida najzastupljenija je metoda konačnih volumena. Rezultat diskretizacije diferencijalnih jednadžbi je sustav algebarskih jednadžbi koje mogu biti

linearne ili nelinearne te ih je moguće riješiti uz pomoć računala. Nelinearne jednadžbe, za razliku od linearnih, zahtijevaju iteracijski postupak rješavanja. Analiza rješenja podrazumijeva prikazivanje i validaciju značajnih skalarnih, vektorskih i tenorskih polja varijabli toka (polja tlaka, brzina, sila, naprezanja, itd.).

Osnovni zakoni dinamike fluida su: zakon očuvanja mase, zakon očuvanja količine gibanja, zakon očuvanja momenta količine gibanja, zakon očuvanja energije te drugi zakon termodinamike. Za slučaj da nema momenata raspodijeljenih po masi i površini materijalnog volumena zakon momenta količine gibanja se svodi na činjenicu simetričnosti tenzora naprezanja, pa ako se ta simetričnost pretpostavi, to znači da je jednadžba momenta količine gibanja već zadovoljena. Entropija se pojavljuje samo u Gibbsovoj jednadžbi i može se rješavati neovisno od ostalih.

Za homogeni idealni plin, može se dati sljedeći sustav jednadžbi:

Zakon očuvanja mase odnosno jednadžba kontinuiteta:

$$\frac{\partial \rho}{\partial t} + \frac{\partial \left(\rho v_j \right)}{\partial x_j} = 0 \tag{1}$$

Jednadžba količine gibanja

$$\frac{\partial \left(\rho v_i \right)}{\partial t} + \frac{\partial \left(\rho v_j v_i \right)}{\partial x_j} = \frac{\partial}{\partial x_j} \left(-p \delta_{ji} + \sum_{ji} \right) + \rho f_i \tag{2}$$

Energetska jednadžba, odnosno jednadžba unutarnje enrgije idealnog plina

$$\frac{\partial \left(\rho c_v T \right)}{\partial t} + \frac{\partial \left(\rho c_v v_j T \right)}{\partial x_j} = -p \frac{\partial v_j}{\partial x_j} + \sum_{ji} \frac{\partial v_i}{\partial x_j} + \frac{\partial}{\partial x_j} \left(\lambda \frac{\partial T}{\partial x_j} \right) + q_H \tag{3}$$

Jednadžba stanja idealnog plina

$$p = \rho R T \tag{4}$$

2. Diskretizacija domene i jednadžbi

Domena strujanja fluida obično je diskretizirana metodom kontrolnih volumena. Domena diskretizirana metodom kontrolnih volumena podijeljena je na N malih volumena koji se nazivaju kontrolni volumeni ili ćelije. Broj, oblik, veličina i distribucija kontrolnih volumena ovisi o vrsti problema koji se pokušava riješiti.

Kontrolni volumen u inercijskom sustavu je volumen koji je stacionaran ili se giba konstantnom brzinom te kroz taj volumen struji fluid. Granice kontrolnog volumena su kontrolne površine i točke na rubovima kontrolne površine nazivaju se čvorovi.

U težištu kontrolnih volumena računaju se svojstva fluida koji struji (brzine, tlakovi, temperature, itd.) pomoću Navier-Stoekesovih jednadžbi. U numeričkim proračunima veličine su poznate samo u točkama domene (težištu kontrolnog volumena, težištu kontrolne površine i čvorovima). Navier-Stokesove jednadžbe potrebno je diskretizirati matematičke operatore kako bi bilo moguće računati sa već postojećim vrijednostima.

Rješavač baziran na tlaku omogućava da se strujanje riješi na segregirani ili spojeni način. Koristeći spojeni način dobivamo robustnu i učinkovitu jedno faznu implementaciju za stacionarni tok, uz bolju učinkovitost u usporedbi s segregirani načinom rješavanja. Dok segregirani rješavač baziran na tlaku rješava momentnu jednadžbu i korekcije tlaka odvojeno, spojeni algoritam rješava momentnu jednadžbu i jednadžbu kontinuiteta zajedno. U momentnoj jednadžbi gradijent tlaka za komponentu k je u formi:

$$\sum_f p_f A_k = - \sum_j a^{u_k p} P_j \tag{5}$$

gdje $a^{u_k p}$ je koeficijent deriviran iz Gaussovog teorema divergencije i sheme interpolacija tlaka. Za i-tu ćeliju diskretizirana forma momentne jednadžbe za komponentu u_k je definirana kao:

$$\sum_j a_{ij}^{u_k u_k} u_{kj} + \sum_j a_{ij}^{u_k p} P_j = b_i^{u_k} \tag{6}$$

U jednadžbi kontinuiteta diskretizirana je kao:

$$\sum_k \sum_j a_{ij}^{p u_k} u_{kj} + \sum_j a_{ij}^{pp} P_j = b_i^p \tag{7}$$

Rezultat sustava jednadžbi u diskretiziranom obliku:

$$\sum_j [A]_{ij} \vec{X}_j = \vec{B}_i \tag{8}$$

3. Numerička analiza brtvi

Da bi se provela numerička analiza prvo je bilo potrebno kreirati geometrijske modele i sklopove modela kako bi dobili domenu kroz koju protječe fluid. Svi geometrijski modeli su prikupljeni osim hula brtve koja je morala biti dizajnirana iz samoga početka. Prikupljeni geometrijski modeli od: belt brtve, gornjeg i donjeg dijela unutarnjeg kućišta komore izgaranja obrađeni su na naći da si im uklonjeni dijelovi koji nisu potrebni ili ne utječu na strujanje fluida odnosno na učinkovitost brtvi. Hula brtva je dizajnirana u softwerskom alatu CATIA. Zatim su svi geometrijski modeli učitani u ANSYS SpaceClaim gdje su se modeli doveli u pravi položaj u odnosu jedan na drugi. Te na kraju u ANSYS Design Modelr-u sklopovi koji čine slučaj s belt brtvom i slučaj sa hula brtvom izrezani su na način da čine periodički model. Iz tih periodičkih modela kreirani su negativi odnosno domene u kojima će strujati fluid. Na Slici 6. može se vidjeti jedan segment belt brtve te belt brtva u sklopu gornjeg i donjeg dijela unutarnjeg kućišta komore izgaranja izrezan kako bi činio periodički model.
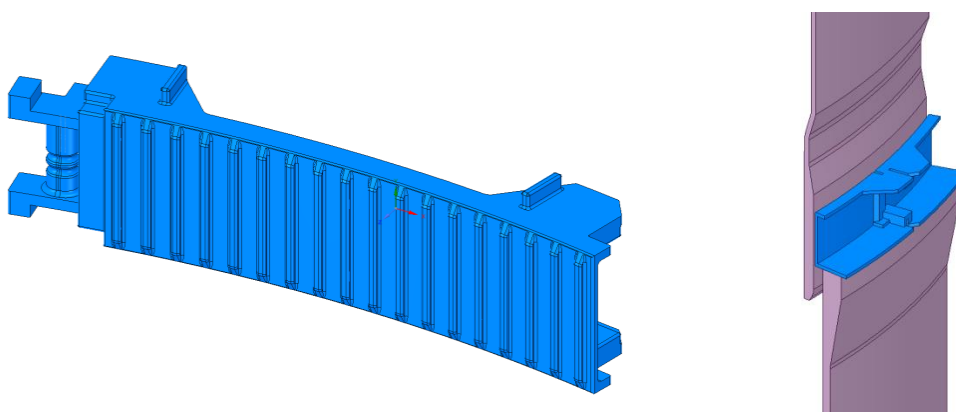
Slika 6. Model jednog segmenta belt brtve i belt brtva sa pripadajućim dijelovima gornjeg i donjeg dijela unutarnjeg kućišta komore izgaranja

Na Slici 7. može se vidjet cijela hula brtva te brtva u sklopu gornjeg i donjeg dijela unutarnjeg kućišta komore izgaranja. Za razliku od belt brtve hula brtva nije segmentirana i cijela je izrađena u jednom komadu.
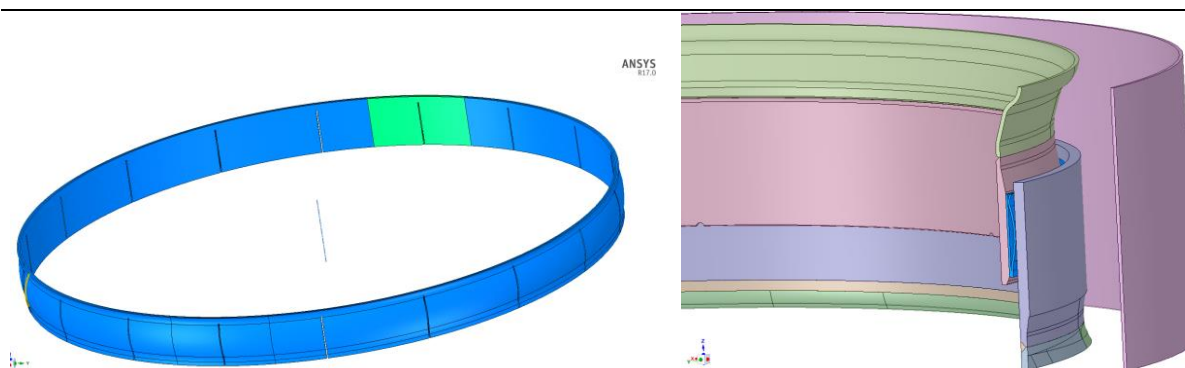
Slika 7. Hula brtva i hula brtva sa pripadajućim dijelovima gornjeg i donjeg dijela unutarnjeg kućišta komore izgaranja

Na Slici 8. može se vidjet cijela belt brtva sastavljena od 18 segmenata te hula brtva koja je izrađena u jednom komadu. Moguće je vidjeti i označeni periodički dio koji će biti podvrgnut numeričkoj analizi. Periodička simulacija moguća je samo ako to dozvoljava geometrija dijelove te ako se struktura strujanja i toplinsko toka periodički ponavlja.
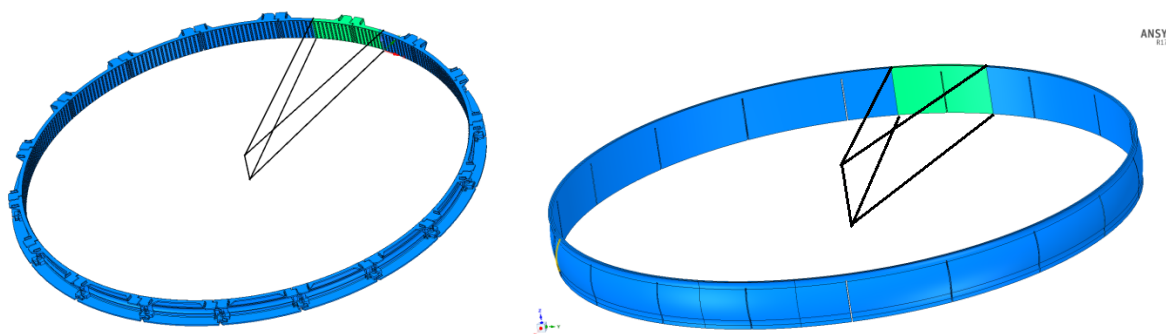
Slika 8. Periodički isječeni dijelovi cijelih brtvi, belt brtve lijevo i hula brtve desno

Kanali za strujanje hladnog zraka i vrućih plinova izrađeni su i mogu se vidjeti na Slika 9 i na Slika 10. Sačinjeni su od gornjeg dijela unutarnjeg kućišta komore izgaranja, belt ili hula brtve i donjeg dijela unutarnjeg kućišta komore izgaranja. Ovi kanali samo su mali dio cijelih kanala kojima struje hladni zrak i vrući dimni plinovi. Na stranicama ovih kanala periodički rubni uvjeti biti će primjenjeni. U modelu korištenom za numeričku analizu kanali su produljeni sa cilindričnim površinama kako bi rubne dijelove domena kao što su ulaz i izlaz fluida, pomaknuli dalje od prostora koji nas interesira kako ne bi utjecali na konačno rješenje.
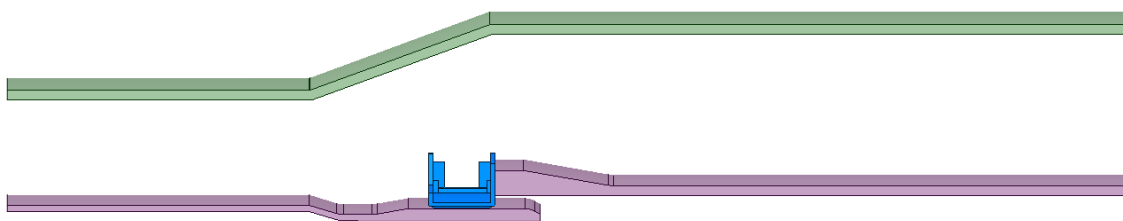
Slika 9. Sklop domene belt brtve proširen cilindričkim površinama
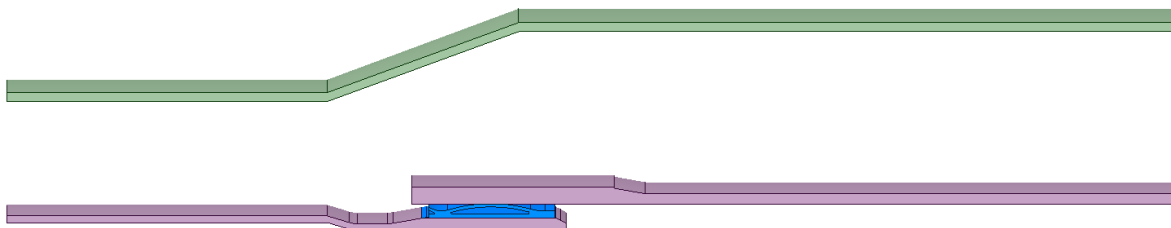
Slika 10. Sklop domene hula brtve proširen cilindričkim površinama

Prijenos topline u fluidu i unutar samih komponenti prostorna diskretizacija ili mreža mora se generirati za oba dijela. Mreža komponenti biti će generirana unutar njih dok će mreža fluida biti generirana na negativu koji predstavlja domenu fluida. Cijela domena može se vidjeti na Slika 11. i na Slika 12..
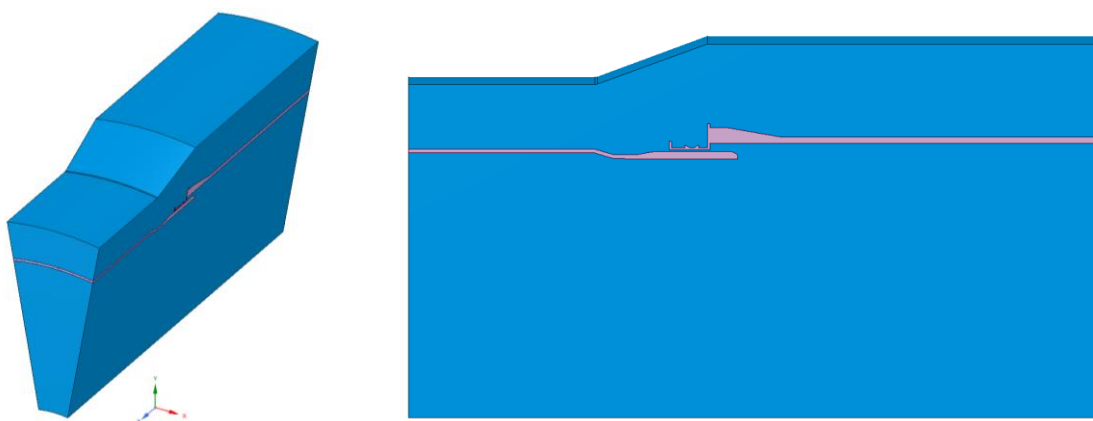
Slika 11. Cijela domena belt brtve na kojoj će biti generirana mreža
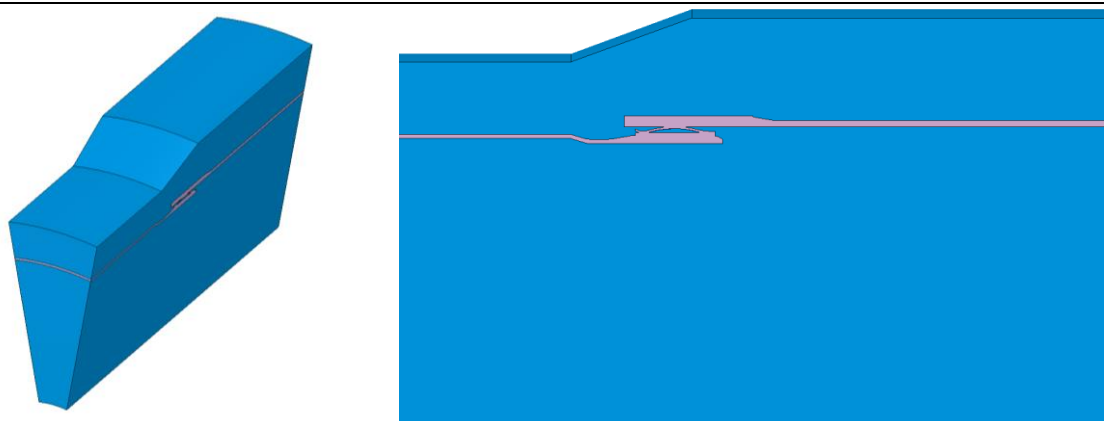
Slika 12. Cijela domena hula brtve na kojoj će biti generirana mreža

Mreža za belt i hula slučaj generirana je u programskom alatu ANSYS ICEM. Prethodno pripremljena geometrija učitana je u ANSYS ICEM gdje su napravljeni zadnji popravci na geometriji kako bi mreža bila što kvalitetnija. Prvo je generirana mreža za negativ domene odnosno za fluid. Zatim je generirana mreža unutar komponenti odnosno za kruti materijal. Na isti način izrađena je mreža za oba slučaja.
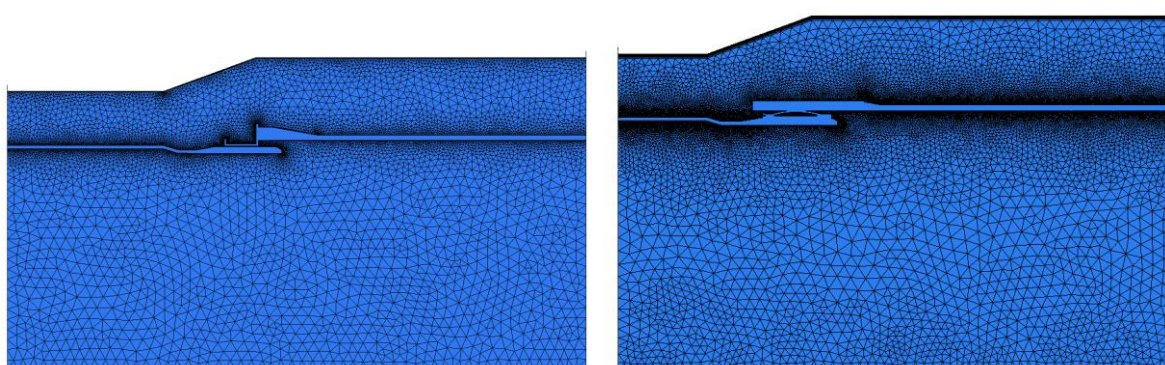
Slika 12. Generirana mreža za slučaj belt brtve lijevo i hula brtve desno

Na domeni belt i hula brtve imamo po dva izlaza i dva ulaza fluida u domenu. Jedan ulaz i jedan izlaz za hladan zrak te jedan ulaz i jedan izlaz za vruče dimne plinove. Ulazi su definirani kao „pressure-inlet" rubni uvjeti dok su izlazi definirani kao „pressure-outlet" rubni uvjeti. Vrijednosti tlakova na izlazu i ulazu u domenu prikazani su u Tablica 1. isto tako na njima su definirane i temperature.

Tablica 1. Tlakovi zadani na ulazu i izlazu

Površine	Rubni uvjeti	Tlak kpa	Temperatura K
Ulaz zraka	Pressure-inlet	1260	650
Izlaz zraka	Pressure-outlet	1240	600
Ulaz dimnih plinova	Pressure-inlet	1215	1400
Izlaz dimnih plinova	Pressure-outlet	1200	1350

Na svim zidovima unutar domene postavljen je no-slip rubni uvjet. Periodičke površine namještene su u parovima sa periodičkim rubnim uvjetima. Površinska mreža na periodičkim parovima je identična. Isto tako površinska mreža koja pripada i fluidu i krutom materijal je identična za obe domene. Na krajnjem donjem dijelu domene primijenjen je symmetry rubni uvjet. Slika 12. prikazuje smjer protjecanja fluida i rubne uvijete koji su primijenjeni da bi ostvario takva tok fluida unutar domene. Hladan zrak nalazi se na vanjskom dijelu domene i struji s desna na lijevo pritom hladeći dijelove domene kako je i prikazano na slici dolje, dok vrući dimni plinovi struje s lijeva na desno pritom zagrijavajući dijelove domene. Dio hladnog zraka proljeće kroz brtvu pri tome osiguravajući hlađenje brtve i hlađenje unutrašnjih dijelova gornjeg i donjeg dijela unutarnjeg kućišta komore izgaranja.
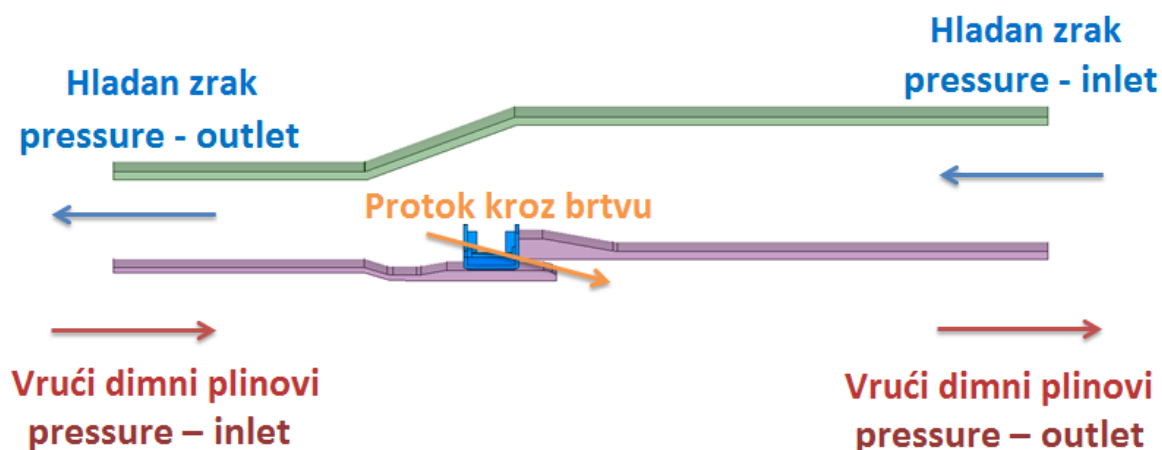
Slika 12. Smjer protjecanja fluida i rubni uvjeti na ulazima i izlazima domene

4. Rezultati numeričke analize

Numerička simulacija provedena je za dva slučaja, belt i hula brtvu. Rezultati numeričke analize dani su u obliku slika, tablica i opisa. Težnja prikaza rezultata je na usporedbi ta dva slučaja. Svi rezultati dobiveni su pomoću ANSYS Fluenta i postprocesirani u ANSYS CFD post alatu.

4.1. Polja tlakova i brzina

Polja statičkog tlaka generirana su za slučajeve belt brtve i hula brtve radi lakše usporedbe strujanja fluida. Viši tlak zraka može se vidjeti na strani hladnog zrake u odnosu tlak na strani vrućih dimnih plinova. Ta razlika u tlaku glavni je pokretač strujanja fluida kroz rupe na brtvama. Isti tlakovi zadani su na rubnim uvjetima za oba slučaja, iz tog razloga slična distribucija tlaka vidljiva je za oba slučaja. Razlike postoje i one se nalaze u području domene uz samu brtvu. Na Slika 13. i na Slika 14. vidljiva su polja tlakova, na lijevoj strani slika prikazan je cijela domena dok je na desnoj strani prikazan uvećan dio domene oko brtvi.

Polja brzina strujanja fluida isto su generirana za oba slučaja, radi lakše usporedbe strujanja fluida. Posljedica razlike tlakova je upravo strujanje fluida brzinama koje su prikazane na Slika 15. i na Slika 16. Iz slika je vidljivo da su najveće brzine postignute upravo u prolazom kroz brtve gdje fluid prestrujava sa strane hladnog zraka na stranu vrućih dimnih plinova. Maksimalne vrijednosti za oba slučaja su oko 115 m/s. Na slikama dolje s lijeve strane nalaze se prikazi presjeka cijele domene dok se s desne strane nalaze slike gdje je uvećano područje oko brvi.
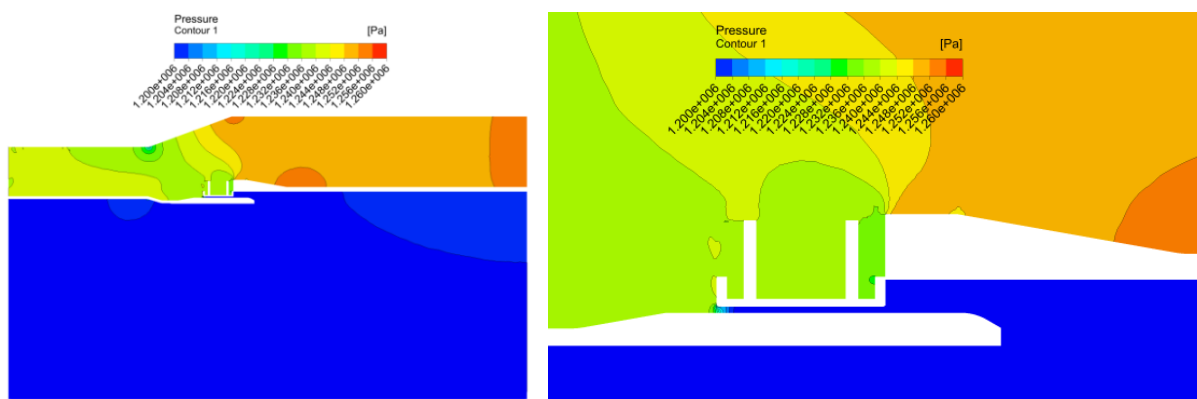
Slika 13. Polje statičkih tlakova belt brtve
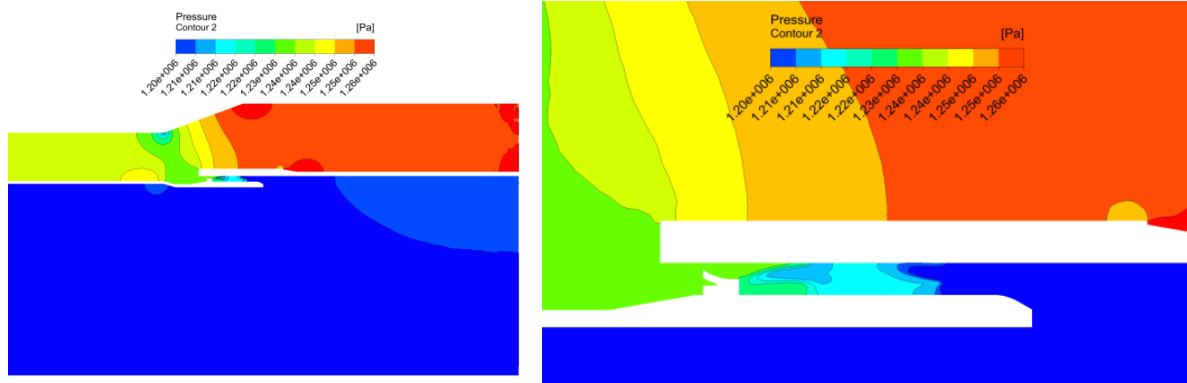
Slika 14. Polje statičkih tlakova hula brtve
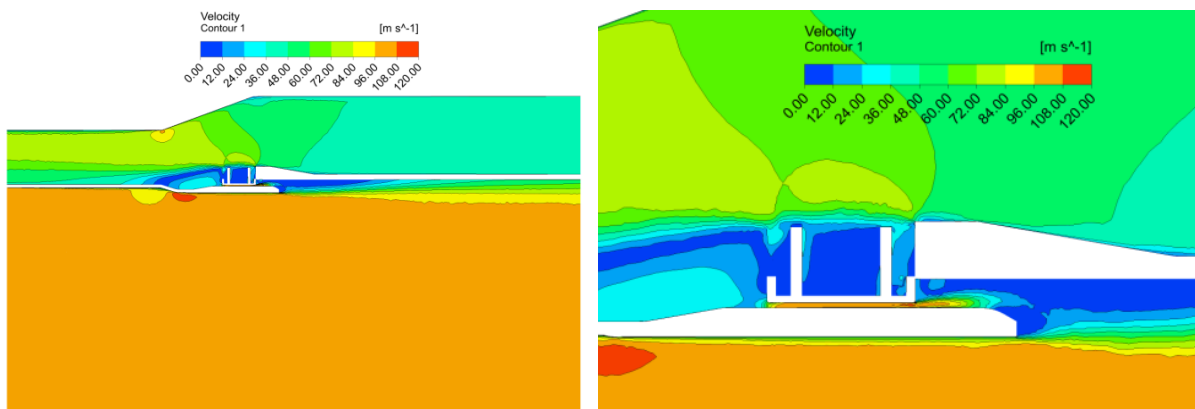
Slika 15. Polje brzina strujanja fluida belt brtve
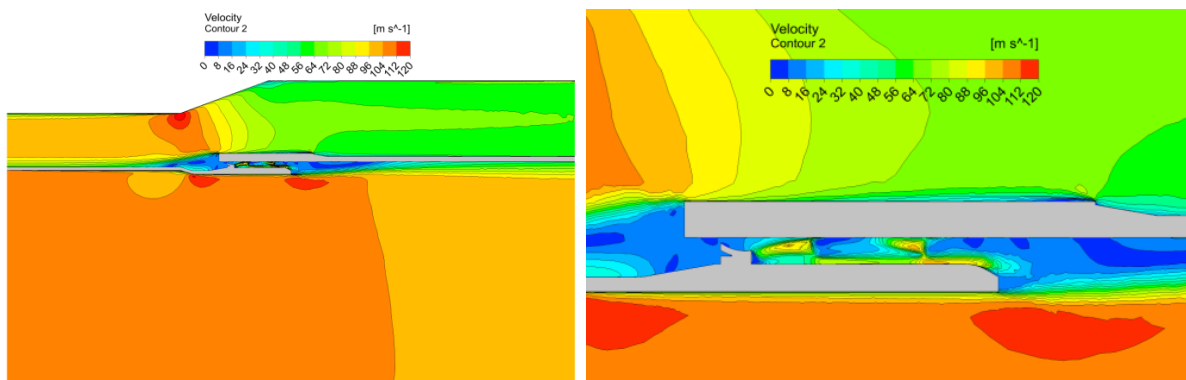
Slika 16. Polje brzina strujanja fluida hula brtve

Na slika 17. i na slika 18. dana su temperaturna polja na površinama krutih tijela, s lijeve strane nalazi se belt brtva dok se s desne strane nalazi hula brtva. Slike prikazuju kako hladan zrak i vrući dimni plinovi utječu na temperature gornjeg i donjeg dijela unutarnjeg kućišta komore izgaranja te brtvi. Najniže temperature vide se upravo na brtvama jer je tamo zbog strujanja hladnog zraka kroz prolaze na brtvama hlađenje najbolje.
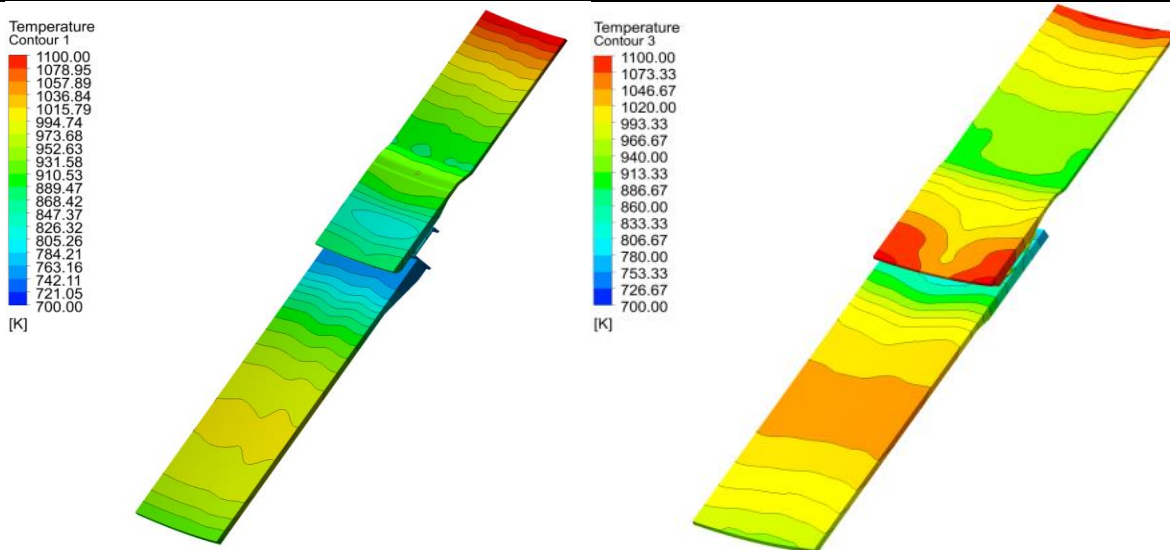
Slika 17. Temperature na površini materijal

Temperature za slučaj hula brtve na donjoj strani gornjeg dijela unutarnjeg kućišta komore izgaranja vrlo su visoke u usporedbi s istim dijelom za slučaj belt brtve. Razloge tome je bolja raspodjela hlađenja kod belt brtve. Na donjem dijelu unutarnjeg kućišta komore izgaranja isto se primjećuju više temperature za hula brtvu u odnosu na belt brtvu, posljedica je to strukture strujanja fluida na strani vrućih dimnih plinova.

4.2. Struktura strujanja fluida

Struktura strujanja fluida za oba slučaja prikazuje se slikama strujnica. Na slika 18. moguće je vidjeti strujnice obojene poljem brzina koje prikazuju strujanje hladnog zraka iz dijela hladnog zraka kroz prolaze na brtvi do dijela sa vrućim dimnim plinovima. Hladni zrak cirkulira prije nego što uđe u prolaze na brtvama. Prolazeći kroz brtve strujanje se ubrzava što se na slikama vidi promjenom boje strujnica. Za slučaj hula brtve postoji i cirkulacijsko strujanje unutar same brtve. Izlaskom iz brtve hladni zrak se počinje cirkularno gibati te se miješa sa vrućim dimnim plinovima. Kod hula brtve to cirkulacijsko gibanje na izlazu iz brtve je puno jače izraženo. Na slikama koje prikazuju strujnice belt brtva nalazi se s lijeve strane dok je hula brtva s desne strane.
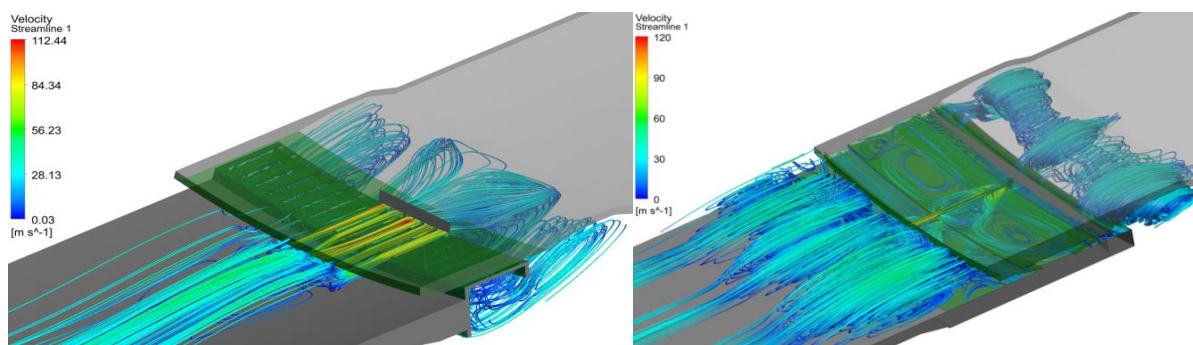
Slika 18. Slike strujnica belt i hula brtve obojene poljima brzina

Cirkulacijsko strujanje hladnog zraka na izlasku iz prolaza kroz brtve puno je jače izraženo za slučaj hula brtve i dobro se može vidjeti na Slika 19 To cirkulacijsko gibanje hladnog zraka povlači dio vrućih plinova prema dolje, što se i može vidjeti na Slika 19 koja prikazuje hula brtvu. Rezultat ovakvog gibanja fluida su povišene temperature gornjeg i donjeg dijela unutarnjeg kućišta komore izgaranja za slučaj hula brtve.
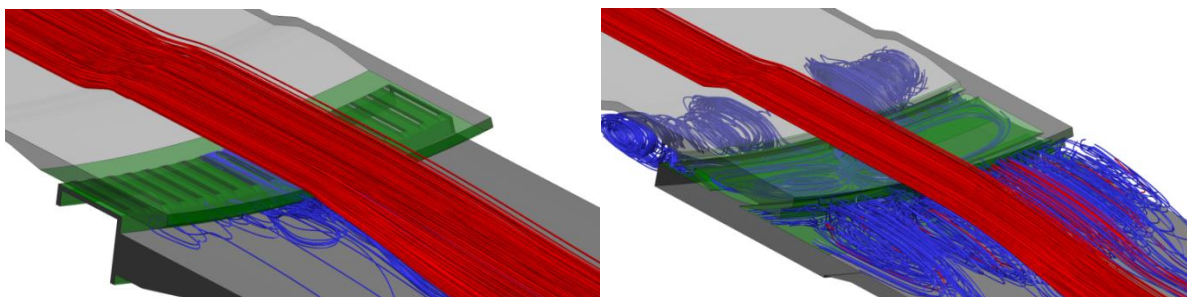
Slika 19. Slike strujnica belt i hula brtve, crveno – vrući plinovi, plavo – hladan zrak

4.3. Maseni protoci

Drugi važni faktor koji je ispitan ovom numeričkom analizom je maseni protok hladnog zraka kroz prolaze na brtvama. Da bi se ostvarila implementacija nove hula brtve u plinskoj turbini koja već radi godinama, maseni protok hladnog zraka koji ide prema komori za izgaranje mora ostati nepromijenjen. Što znači maseni tok kroz prolaze na belt brtvi i hula brtvi mora biti jednak za određene radne uvijete plinske turbine. U sklopu ovog rada ispitano je samo jedno stanje rada plinske turbine. Rezultati masenih protoka mogu se vidjeti u Tablici 2. Iz te tablice možemo zaključiti da geometrijske promjene napravljene da bi se hula brtva uspjela ugraditi na mjesto belt brtve mjenja protok hladnog zraka koji ide prema komori za izgaranje. Protok kroz prolaze na hula brtvi manji je u odnosu na belt brtvu. Smanjujući maseni protok

kroz brtvu smanjuje se hlađenje sučelja i same brtve što za posljedicu ima veće temperature gornjeg i donjeg dijela unutarnjeg kućišta komore izgaranja.

Tablica 2. Maseni protoci

Maseni protoci						
Sub-model				Cijeli model		
	Belt Brtva	**Hula Brtva**		**Belt Brtva**	**Hula Brtva**	
Ulaz zraka	15.17	14.69	kg/s	273.06	264.4	kg/s
Izlaz zraka	14.93	14.49	kg/s	268.74	260.8	kg/s
Ulaz plina	22.07	21.21	kg/s	397.26	381.8	kg/s
Izlaz plina	22.32	21.4	kg/s	401.76	385.2	kg/s
Protok kroz brtvu	**0.24**	**0.18**	**kg/s**	**4.32**	**3.24**	**kg/s**

5. Zaključak

Usporedba belt i hula brtve prikazana je u prethodnom poglavlju. Učinkovitost hlađenja može se usporediti na slikama sa konturama temperatura na unutarnjem kućištu komore izgranja. Proučavajući konture temperatura na površini kućišta može se zaključiti da hula brtva ima slabiju učinkovitost hlađenja u odnosu na belt brtvu. Najveća razlika uočava se na donjem dijelu gornjeg dijela unutarnjeg kućišta komore izgaranja. Isto tako na donjem dijelu unutarnjeg kućišta komore izgaranja uočava se područje povišenih temperatura kod slučaja hula brtve u odnosu na slučaj s belt brtvom. Mjesta povišenih temperatura na komponentama imaju veliki utjecaj na životni vijek dijelova turbine.

Očekivana poboljšanja primjenom hula brtve su: jeftinija izrada, jednostavnija i brža montaža, bolje hlađenje komponenata i dulji životni vijek komponenata. Ukoliko hula brtva nema zadovoljavajuću učinkovitost hlađenja neće se ostvariti gore navedena poboljšanja. Temeljem rezultata možemo zaključiti da Hula brtva koja je numerički analizirana u ovome radu ne zadovoljava učinkom hlađenja.

Tri su razloga zašto hula brtva ne zadovoljava učinkom hlađenja:

Prvi je recirkulacija fluida nakon izlaska iz prolaz kroz brtvu koja povlači vruće dimne plinove prema površini kućišta komore izgaranja što za posljedicu ima povećanje temperature same komponente. Druga je smanjenje masenog protoka u odnosu na slučaj belt brtve. Treći

razlog je mali broj prolaza zraka na hula brtvi u usporedbi s belt brtvom. Rezultat toga su lokalne visoke temperatura gornjeg dijela unutarnjeg kućišta komore izgaranja.

Da bi se povećala učinkovitost hlađenja trebalo bi povećati broj prolaza na samoj hula brtvi. Pritom smanjujući širinu pojedinog prolaza kako bi se ostvario optimalni maseni protok odnosno identičan protok kao kod belt brtve. Time bi se dobila bolja raspodjela hlađenja koja bi za posljedicu imala nestajanje lokalnih visokih temperatura na gornjem dijelu unutarnjeg kućišta komore izgaranja. Isto tako s povećanjem prolaza kroz brtvu problem recirkulacije fluida bi se umanjio. Rezultati dobiveni u ovom radu mogu se koristi pri budućim analizama hula brtvi s više prolaza kako bi se ustanovio utjecaj povećanja broja prolaza kroz brtvu na strujanje fluida i učinkovitost hlađenja.

Abstract

This thesis deals with large-scale cylindrical interface sealing between the hot gas path components of silo combustion chamber. Implementation of hula seal for replacing old belt seal will be checked in order to minimize the amount of cooling and leakage air, without negative impact on the lifetime of the components. Hula seal is annular flexible spring finger seal used to compensate misalignment between co-annular parts, while providing effective sealing performance. It is circumferential metal seal that is slotted in the axial direction and contoured to be spring-loaded between inner and outer diameter of the matching parts that experience relative axial motion. Long term successful implementation of the hula seal for sealing of stationary interfaces for industrial and aero gas turbine engines confirms benefits like improved lifetime of the hot gas parts, reduction of manufacture costs and on-site assembly time. The target engine type is older gas turbine that currently uses belt seal as seal for cylindrical interface between the hot gas path components of silo combustion chamber. Main reason of choosing this engine is the highest wear impact and costs of the belt seal compared to other engines.

In scope of this thesis computational fluid dynamics method is used to verify the sealing performance of the hula seal and compare it with belt seal performance. Models of belt seal, combustion inner liner and hot gas casing that are used already existed, while hula seal model was designed by descriptions from patent. From this models, assembly of two cases were made, one for belt seal case and one for hula seal case. Periodic models were created from assembly models to reduce mesh generation and computational time. Numerical analysis solved conjugate heat transfer problem which means that along fluid flow, heat transfer interaction between fluid and solid was solved as well. Result which shows fluid flow and thermal condition of fluid and solid are presented. Based on result it is concluded that performance of hula seal model used in this thesis are not good enough. Compared to belt seal hula seal cooling performances are worse. Suggestions for improving hula seal performance were given.

Key words:

Hula seal, Gas turbine, Computational fluid dynamics, Numerical analysis, Combustion chamber, Conjugate heat transfer

1. Introduction

1.1.   Motivation

Old gas turbines that are still in use can be upgraded by newly developed components. When life cycle of old components comes to end it is replaced by new if possible better components. Newly developed components usually do their job better or as good as old components and are cheaper to manufacture and montage. Main reason to categorize new ones as better is that they provide longer life time. A leakage through the sealing of interface is the parameter that will be compared. Two types of sealing were considered: current standard called belt seal and new one called hula seal. The old belt seal will be numerically analyzed to get better understanding of flow structure and to compare belt seal numerical analysis results with results of new hula seal. The main reason for numerical simulation study is to analyze cooling characteristics of hula seal interface for gas turbine that currently uses old belt seal. For better understanding and easier comparison of seals results will contain temperature fields, mass flow rate and 3d flow structure. The evaluation of implementation of hula seal base on numerical analysis will provide guidelines for increasing performance. Guidelines will contain suggestions for hula seal geometry improvements like increasing or decreasing gaps for leakage. Based on the results of numerical calculation the hula seal potential of improvement will be evaluated.

1.2.   Gas turbines

A gas turbine is a combustion engine that can convert natural gas or other liquid fuels to mechanical energy. This energy then drives a generator that produces electrical energy.
To generate electricity, in the gas turbine a mixture of air and fuel burns at very high temperatures, causing the turbine blades to spin. The spinning turbine drives a generator that converts the energy into electricity. The gas turbine can be used in combination with a steam turbine - in a combined-cycle power plant - to create power extremely efficiently.
The gas turbine compresses air and mixes it with fuel forming air-fuel mixture that is ignited and then burned at extremely high temperatures, creating a hot gas. The hot air-and-fuel mixture moves through blades in the turbine, causing them to spin quickly. The fast-spinning turbine blades rotate the turbine shaft. Turbine shaft rotation powers the generator. The

spinning turbine is connected to the rod in a generator that turns a large magnet surrounded by coils of copper wire. Generator magnet causes electrons to move and creates electricity. The fast-revolving generator magnet creates a powerful magnetic field that lines up the electrons around the copper coils and causes them to move. The movement of these electrons through a wire is electricity.
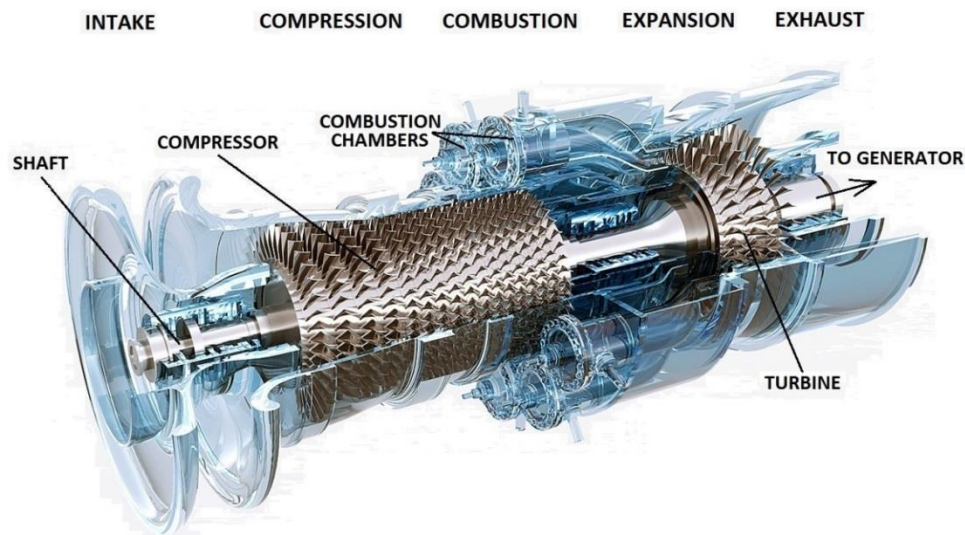
Figure 1.   Gas turbine

1.3.   Silo combustor gas turbine

In this chapter working principle of silo combustor engine is described. Air form outside is drawn by compressor at the right side of Figure 2. Air is then compressed in several stages, and then it flows up just inside the wall of the large cylinder at the center, outside of hot gas casing. This pre-heats the combustion air while keeping the hot gas casing and the combustion inner liner cool and preventing it from melting. The air is blended with natural gas (or fuel oil) at the top of the silo combustor. The fuel/air mixture is burned as it travels down in the silo inside combustion inner liner, then the hot gases are routed into a donut called the hot gas casing that spreads them all around the turbine shaft, where they are allowed to expand and drive the turbine.
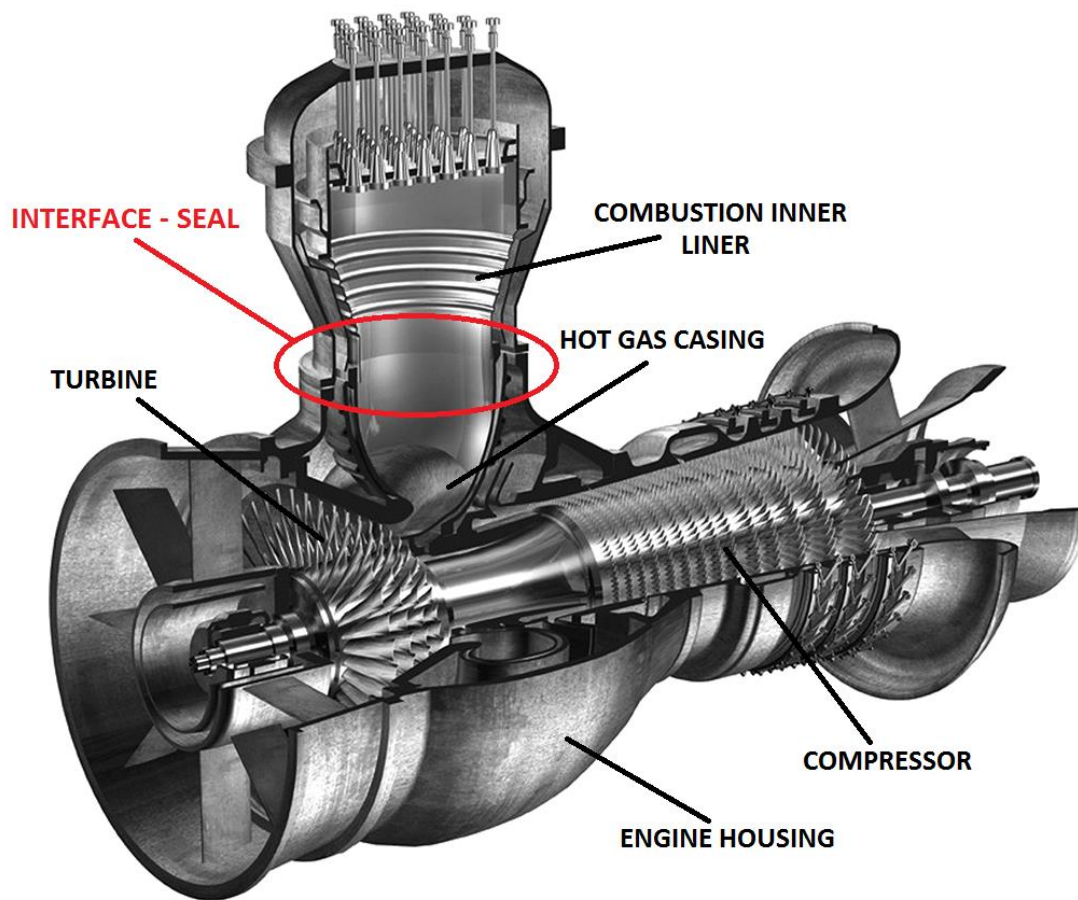
Figure 2.   Silo combustor gas turbine

1.4.   Hot gas casing and combustion inner liner

Gas turbine power plant consists of a gas turbine, an air compressor, and a combustion chamber. Main part of combustion chamber is a combustion space which is enclosed by a combustor inner liner (CIL) and a hot gas casing (HGC). The gas turbine, the compressor, and the combustion chamber are enclosed in engine housing. While in operation the gas turbine is supplied with hot gases form the combustion chamber. Compressed air supplied by the compressor flows into the combustion chamber through a space located between the hot gas casing and the engine housing. Because this compressed air has a lower temperature then the surface of the hot gas casing, the air is absorbing heat. So we can say that hot gas casing is cooled by the compressed air. After cooling hot gas casing compressed air is streaming outside combustion inner liner, cooling it as well and at the end entering combustion chamber. Combustion Inner Liner is part of combustion chamber which separates cool air from hot

gases. In combustion chamber fuel is injected in to stream of air. Fuel mixed with air burns and generates heat. Mixture of hot gases then exits combustion chamber and enters hot gas casing. Because of very high temperatures of hot gases inside combustion inner liner and hot gas casing it is necessary to provide cooling for these parts. From hot gas casing, hot gases are entering turbine. The method used to cool the hot gas casing of engine leads to a non-uniform flow of cooling compressed air over the hot gas casing and combustion inner line. This non-uniform flow produces non-uniform wall temperatures which lead to thermal wall stresses, particularly when the turbine inlet temperatures are high. Such thermal stresses can lead to cracks in hot gas casing and combustion inner liner. [11]

Figure 3.   Hot gas casing and combustion inner liner

1.5.   Seal between hot gas casing and combustion inner liner

In the older engines (gas turbines) combustor inner liner (CIL) and hot gas casing (HGC) were installed with overlap and did not have any sealing in-between. In engines with side positioning of combustor similar design have ducts and joints used for sealing. At the end of 1970th the sealing consisting of segments attached to the inner liner was developed. The design is called "Monthey seal" and it is still installed in some older gas units that are working today. The leakages through the gap between segments generate hot gas ingestion and local overheating on the inner liner and hot gas casing. This phenomenon was identified shortly after implementation of "Monthey seal and because of that development of new sealing was initiated. The new seal, which is called the belt seal, has been developed in several steps, and since beginning of 1990th it became a standard for engines with silo combustor.

The Belt seal improved the situation and in some units phenomenon of hot gas ingestion and local overheating on the inner liner and hot gas casing was reduced, i.e. the oxidation due to overheating is not so strong anymore. However, in some units phenomenon of hot gas ingestion and local overheating on the inner liner and hot gas casing is still visible, which means that belt seal still need to be improved. In the past further investigations of phenomenon of hot gas ingestion and local overheating on the inner liner and hot gas casing were undertaken and modification of belt seal (improved mechanical design) have been done.
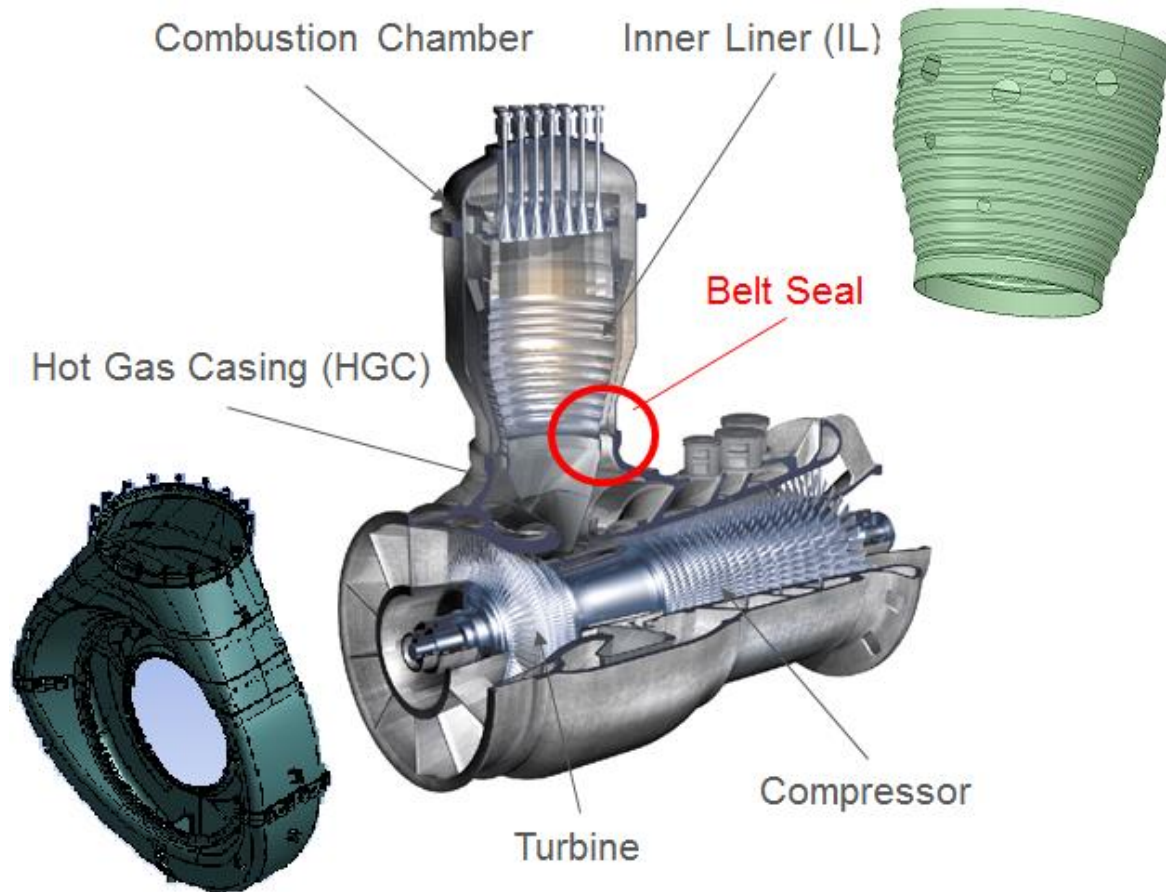
Figure 4.   Belt seal location in silo combustor gas turbine

Today standard belt seal for gas turbine with silo combustor is being replaced with new technology, Hula seal. Some manufactures of gas turbines have long years of successful implementation of Hula Seal for sealing of stationary interfaces for industrial and aero-derivative engines (interfaces up to ø300-400). Expected benefits from the application of hula seal are: improved lifetime of the hot gas casing and inner liner, reduction of manufacturing costs and on-site assembly time.
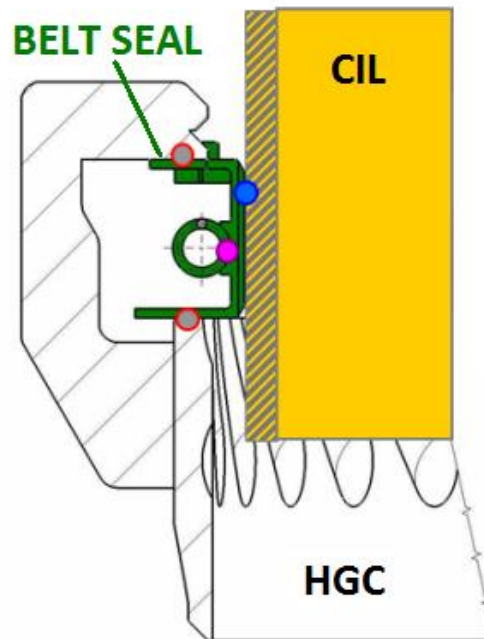
Figure 5.   Interface of: Inner liner – Hot gas casing, sealed with Belt Seal

1.6.   Belt Seal

Belt seal is type of seal used between two parts in combustor section of gas turbines, hot gas casing and combustion inner liner. It consists of the same segments that are banded together with springs. Number of segments of belt seal depends of size of each segment and size of interface between hot gas casing and combustion inner liner. Belt seal which is used in this thesis has 18 segment and diameter of hot gas casing at interface is 1,4 m. On the Figure 6 we can see how one segment of belt seal look like and also we can see belt seal mounted on the hot gas casing. It minimizes leakages of cooling air passing to inner side of combustor parts, still some controllable leakage is essential to cool seal itself and inner side of hot gas casing as well as bottom part of combustion inner liner. As stated earlier the belt seal, has been developed in several steps, and since beginning of 1990th it is a standard for engines with silo combustor. The main problem of this seal is phenomenon of hot gas ingestion and local overheating on the inner liner and hot gas casing and the oxidation due to overheating which has impact on the lifetime of the hot gas casing, combustion inner liner and belt itself. The challenge is to improve lifetime of these parts, reduce manufacturing costs and on-site assembly time of the seal. [4

Figure 6.   Segment of belt seal and belt seal mounted on Hot Gas Casing

1.7.   Hula seal

A few companies that manufacture combustion part for gas turbines use a hula seal as an interface seal between the combustion inner liner and the hot gas casing. Similar types of hula seals may be used between a combustion liner cap assembly and the combustion liner and/or elsewhere with the gas turbine engine. In this thesis standard belt seal is being replaced with new hula seal. As described in patent, commonly owned U.S. Pat. No. 6,334,310, a hula seal is generally defined as a system of leaf springs formed into a round loop and used to seal a sliding interface joint or annular gap between two concentric ducts. [1]

A certain amount of mass flow is generally leaked through the hula seal in order to cool seal itself and interface parts, in our case hot gas casing and combustion inner liner. Maintaining low temperatures about the seals is main function of hula seal. A hula seal with a larger leakage area may be used to divert more airflow directly to the hot side of the liner so as to reduce the air mass flow going to the combustion chamber. This flow also may help increase cooling of hula seal and parts around it. Increasing airflow that passes thru hula seal have positive impact on lifetime of seal itself, hot gas casing and combustion inner liner, but it decrease airflow going to combustion chamber. To maintain airflow that is needed in combustion chamber, flow of air need to be increased by compressor or decrease gaps on hula seal. Focus of this thesis numerical analysis is to compare cooling and impact on mass flow by replacing belt seal with hula seal.

Design of hula seal can vary depending on geometry of interface itself and cooling requirements of interface part. In this case most important parameter is cooling of interface parts, hot gas casing and combustion inner liner as well as hula seal itself to provide longer

lifetime of those parts. Cooling performance is defined by number of gapes on hula seal and their size which defines mass flow of air for cooling. Amount of air mass flow that passes through gaps of hula seal must satisfy certain mass flow so it doesn't compromise performance of gas turbine.

Figure 7.   **Hula seal**

1.8.   Thesis Outline

The main goal of this thesis is comparison of performances for different seal models, by studying results of numerical simulations for both seals. The work covered by this thesis is divided into chapter as follows: In chapter 2, Mathematical Model, deals with used partial differential equations. In chapter 3, entitled Numerical Analysis of Interface Seal, deals with creation of geometry and mesh generation also setup of case is describe. In chapter 5, results obtained by numerical simulations are presented and comparison of interface seals performance is given. In the last chapter 6, conclusion of thesis and guidelines for increasing of hula seal performance are given.

2. Mathematical Model

Fluid flow is described by Navier-Stokes equations. There is no analytical solution of the general form for this equation because of their nonlinear nature. To get some solutions it is important to introduce some simplifications. Therefore for some generic types of flow it is possible to get analytical solution. Today form and characteristics of fluid flow for engineering problems is possible to obtain only by mean of experiment or by numerical analysis. Numerical analysis is done in several steps:

- Selection of mathematical model

- Numerical solution of mathematical model

  - Discretization of flow domain

  - Discretization of mathematical model equations

  - Solution of system of algebraic equations

- Analysis of solution

Mathematical model is system of partial differential equations that are describing physical problem. Calculation of mathematical model demands that domain is discretized, sub-divided into a number of smaller, non-overlapping sub-domains. This sub-division of domain is called a grid or a mesh of cells or control volumes (or elements). Discretization of equation is done by one of methods: Final Difference Method, Finite Element Method or Finite Volume Method. Most commonly used for fluid dynamic analysis is finite volume method. The result of discretization of equations is system of algebraic equations which can be linear or nonlinear equations but there are possible to solve by computers. Difference between linear and nonlinear equation is that nonlinear equation need iterative process of solving that is done by computer.

Analysis of results of numerical simulation includes validations and representation of scalar, vector and tensor fields of flow variables (field of pressure, velocity, forces, temperatures etc.). [2][6]

2.1. Generic scalar transport equation

Generic scalar transport equation can be expressed in standard form as:

$$\frac{\partial \rho \emptyset}{\partial t} + \nabla \cdot (\rho u \emptyset) = \nabla \cdot (\Gamma \nabla \emptyset) + S_\emptyset \tag{1}$$

Where $\emptyset$ is the transported scalar variable, u is the convective velocity and Γ is the diffusion coefficient or diffusivity.

- $\frac{\partial \rho \emptyset}{\partial t}$ is the transient term, it accounts for the accumulation of $\emptyset$ in the control volume

- $\nabla \cdot (\rho u \emptyset)$ is the convection term, it account for the transport of $\emptyset$ due to the existence of the velocity field

- $\nabla \cdot (\Gamma \nabla \emptyset)$ is the diffusion term, it accounts for the transport of $\emptyset$ due to its gradients

- $S_\emptyset$ is the source term, it account s for any sources or sinks that either crate or destroy $\emptyset$, and any extra terms that cannot be cast into convection or diffusion term

The objective of all discretization techniques (Finite Difference, Finite Element, Finite Volume, Boundary Element...) is to devise a mathematical formulation to transform each of these terms into an algebraic equation. Once applied to all control volumes in a given mesh, we obtain a full linear system of equations that needs to be solved. [7]

2.2. Conservation form of basic laws of fluid mechanics

Basic laws of fluid mechanics are: Mass conservation law, Conservation of momentum, Energy conservation law and second law of thermodynamics. For case that there is no momentum distributed on mass and surface of material volume momentum conservation law is reduced on fact of symmetry of the stress tensor. If that symmetry is presupposed momentum equation is already satisfied. Entropy appears only in Gibbs equation and it can be calculated separately. [3]

For homogenous ideal gas, system of next equations is worth:

Mass conservation law or equation of continuity:

$$\frac{\partial \rho}{\partial t} + \frac{\partial \left(\rho v_j \right)}{\partial x_j} = 0 \tag{2}$$

Momentum equation:

$$\frac{\partial \left(\rho v_i \right)}{\partial t} + \frac{\partial \left(\rho v_j v_i \right)}{\partial x_j} = \frac{\partial}{\partial x_j} \left(-p \delta_{ji} + \Sigma_{ji} \right) + \rho f_i \tag{3}$$

While for compressible flow with neglect of volume viscosity:

$$\sum_{ji} = \mu \left(\frac{\partial v_j}{\partial x_i} + \frac{\partial v_i}{\partial x_j} \right) - \frac{2}{3} \mu \frac{\partial v_k}{\partial x_k} \delta_{ji} \tag{4}$$

Energy equation, in this case internal energy equation for ideal gas:

$$\frac{\partial \left(\rho c_v T \right)}{\partial t} + \frac{\partial \left(\rho c_v v_j T \right)}{\partial x_j} = -p \frac{\partial v_j}{\partial x_j} + \sum_{ji} \frac{\partial v_i}{\partial x_j} + \frac{\partial}{\partial x_j} \left(\lambda \frac{\partial T}{\partial x_j} \right) + q_H \tag{5}$$

where q_H is density of heat source divided by volume.

Thermal state equation for ideal gas:

$$p = \rho R T \tag{6}$$

where R is specific gas constant and T is absolute temperature.

2.3. Turbulence modeling

Turbulence or turbulent flow is irregular, disorderly, non-stationary, three-dimensional, highly non-liner, irreversible stochastic phenomenon. Characteristic of turbulent flows are: Randomness, Vorticality, Non-linearity and three-dimensionality, Continuity of Eddy Structure, Energy cascade, irreversibility and dissipativeness, Intermittency, High diffusivity, Self-preservation and self-similarity. Turbulent flow is completely understood and described in all its detail: turbulent fluid flow is strictly governed by Navier-Stokes equations. Because of Navier-Stokes equation we understand how turbulence spans wide spatial and temporal scales. When described in terms of vortices, non-linear interaction is complex. Because of non-linear interactions and correlated nature, it cannot be solved statistically. It is not easy to assemble the results of full turbulent interaction and describe them in a way relevant for engineering simulations we are more interested in mean properties of physical relevance.

In spite of its complexity, there is a number of analytical, order-of-magnitude and quantitative results for simple turbulence flows. Some of them are extremely useful in model formulation. Mathematically, after more than 100 year of trying, we are nowhere near to describing turbulence the way we wish. [5]

Properties of turbulence in practices are sometimes desirable and sometimes not. In scope of turbulence problems process of laminar-turbulent transition should be mentioned. It is process in which flow from laminar without outer influence becomes turbulent. This process can be observed on flow over flat plate. [3]
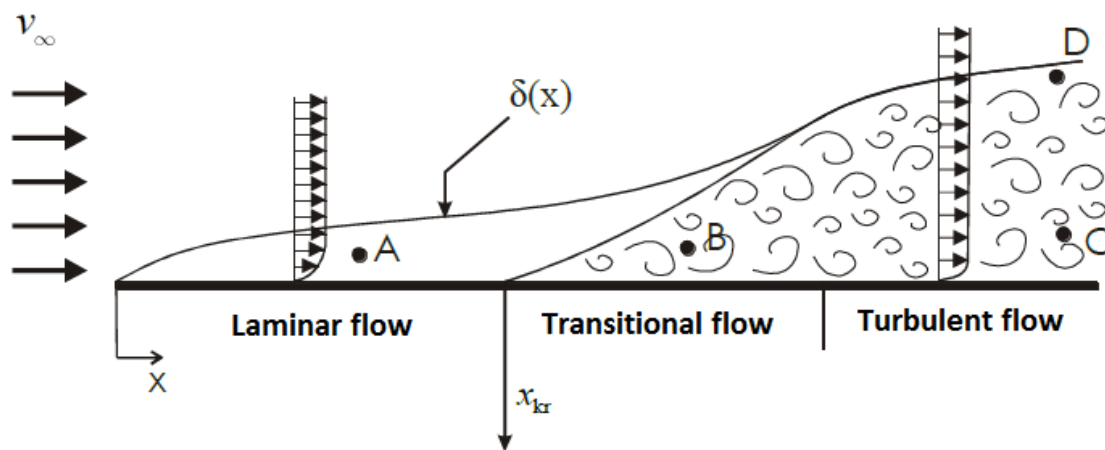
Figure 8. Development of boundary layer over a flat plate including the transition from a laminar to turbulent boundary layer

Turbulence modeling is the construction and use of a model to predict the effects of turbulence. A turbulent fluid flow has features on many different length scales, which all interact with each other. A common approach is to average the governing equations of the flow, in order to focus on large-scale and non-fluctuating features of the flow. However, the effects of the small scales and fluctuating parts must be modeled.

2.3.1. Calculating Turbulance

There are several approaches to numerical modeling of turbulent flow: Direct Numerical Simulation (DNS), Large Eddy Simulation (LES) and statistical approach Navier-Stokes (NS).

A direct numerical simulation (DNS) is a simulation in computational fluid dynamics in which the Navier–Stokes equations are numerically solved without any turbulence model. This means that the whole range of spatial and temporal scales of the turbulence must be solved. All the spatial scales of the turbulence must be resolved in the computational mesh, from the smallest dissipative scales (Kolmogorov microscales), up to the integral scale L, associated with the motions containing most of the kinetic energy. Therefore, the computational cost of DNS is very high. For most industrial applications, the computational resources required by a DNS would exceed the capacity of the most powerful computers currently available. However, direct numerical simulation is a useful tool in fundamental research in turbulence. [7]

Large eddy simulation (LES) is a simulation in computational fluid dynamics where space filter is introduced. Filter separates large eddies form small ones. Large eddies are those which can be solved by assign mesh. Small eddies must be modeled. Logic behind this

approach is that small eddies are easier to model. Increasing resolution of mesh smaller and smaller eddies are being modeled until we get close to direct numerical simulation (DNS).

Third and alternative approach in turbulence modeling is statistical. By separating current values of local flow variable on mean values and fluctuation around mean value it is possible to obtain equations in which unknowns are mean values of flow variables. In case of uncompressible flow averaging of Naver-Stokes equations is conducted by Reynolds averaging and we get (RANS) Reynold Averaged Navier-Stokes equations. The Navier–Stokes equations govern the velocity and pressure of a fluid flow. In a turbulent flow, each of these quantities may be decomposed into a mean part and a fluctuating part. Averaging the equations gives the Reynolds-averaged Navier–Stokes (RANS) equations, which govern the mean flow. However, the nonlinearity of the Navier–Stokes equations means that the velocity fluctuations still appear in the RANS equations, in the nonlinear term from the convective acceleration. This term is known as the Reynolds stress. Its effect on the mean flow is like that of a stress term, such as from pressure or viscosity. To obtain equations containing only the mean velocity and pressure, we need to close the RANS equations by modelling the Reynolds stress term as a function of the mean flow, removing any reference to the fluctuating part of the velocity. This is the closure problem. [9][10] In case of compressible flow Favre averaging is used for averaging Navier-Stokes equations. Averaged Navier-Stokes equations can be written as:

$$
\frac{\partial}{\partial t}
\begin{bmatrix} \rho \\ \rho u_i \\ \rho E \end{bmatrix}
+ \frac{\partial}{\partial x_j}
\begin{bmatrix} \rho u_j \\ \rho u_j u_i + p\delta_{ij} \\ \rho u_j h \end{bmatrix}
- \frac{\partial}{\partial x_j}
\begin{bmatrix} 0 \\ \tau_{ij} + \tau_{ij}^R \\ \left(\tau_{ij} + \tau_{ij}^R\right) u_j - q_i - q_i^R \end{bmatrix}
=
\begin{bmatrix} 0 \\ \rho f_i \\ W_f + S_E \end{bmatrix}
\qquad \textbf{(7)}
$$

Where $\tau_{ij}^R = -\overline{\rho u_i' u_j'}$ is Reynolds stress tensor, $q_i^R = -\overline{\rho h' u_i'}$ is vector of turbulent flow. Other variable are averaged variables of flow. During averaging of equations second order correlation appears: τ_{ij}^R and q_i^R. To solve all unknowns, new equations had to be introduced because system of averaged Navier-Stokes equations isn't closed. This is the closure problem. The problem is fixed by modeling turbulence. There are two basic approaches to statistic turbulent modeling: calculating transport equations for Reynolds stress tensor or Boussinesq approximation.

$$\tau_{ij}^{R} = -\overline{\rho u_i' u_j'} = \mu_t \left(\frac{\partial \overline{v_i}}{\partial x_j} + \frac{\partial \overline{v_j}}{\partial x_j} \right) - \frac{2}{3} \rho \overline{k} \delta_{ij} \tag{8}$$

where μ_t is coefficient of turbulent viscosity which isn't physical property of fluid but function of flow conditions. Coefficient of turbulent viscosity μ_t at laminar flow is equal to zero. Models based on this assumption are called Newtonian turbulence models. [2]

2.3.2. Turbulence models

- $k - \epsilon$ turbulence model

  The $k - \epsilon$ model of turbulence is one of most common turbulence model used today. It is a two equation model and that means it includes two extra transport equations to represent the turbulence properties of the flow. This use of two equations allows accounting for history effects like convection and diffusion of turbulence energy.

  The first transported variable is turbulence kinetic energy k. The second transported variable is the turbulent dissipation ϵ. It is the variable that determines the scale of the turbulence, whereas the first variable k determines the energy of turbulence.

  Usual $k - \epsilon$ models:

  1. Standard $k - \epsilon$ model
  2. Realizable $k - \epsilon$ model
  3. RNG $k - \epsilon$ model

$$\mu_T = \rho C_\mu \frac{k^2}{\epsilon} \tag{9}$$

  where C_μ is predefined constant.

- $k - \omega$ turbulence model

  The $k - \omega$ turbulence model is one of the most commonly used turbulence model. It is a two equation model and that means it includes two extra transport equations to represent the turbulence properties of the flow. This use of two equations allows accounting for history effects like convection and diffusion of turbulence energy.

  The first transported variable is turbulence kinetic energy k. The second transported variable in this case is the specific dissipation ω. It is the variable that determines the scale of the turbulence, whereas the first variable k determines the energy of turbulence.

Usual $k - \omega$ models:

1. Wilcox's $k - \omega$ model
2. Wilcox's modified $k - \omega$ model
3. SST $k - \omega$ model

$$\mu_T = \alpha_\omega \frac{\rho k}{\omega} \tag{10}$$

Where α_ω is correction factor.

Generally turbulence models are divided by number of unknown which are used to describe turbulent viscosity μ_T. Models described above are models with two equations but there are also algebraic models with zero unknowns like Baldwin-Lomax, models with one equation like Spalatal-Allmaras or models with more than two equations like Reynolds stress model.[7]

2.4. Wall functions

Turbulent models describe flow in which turbulent viscosity coefficient μ_T has significantly higher value compared to molecular viscosity coefficient μ. Problem occurs in fluid flow close to sold (wall) surface which suppress oscillations in direction of surface normal and where no-slip condition is set which suppress oscillations of flow velocity in tangential direction relative to the surface. Wall impacts has consequences on fluid flow in boundary layer in which reduction of turbulent energy occurs and with that increase of molecular viscosity compared to turbulent viscosity. [12]
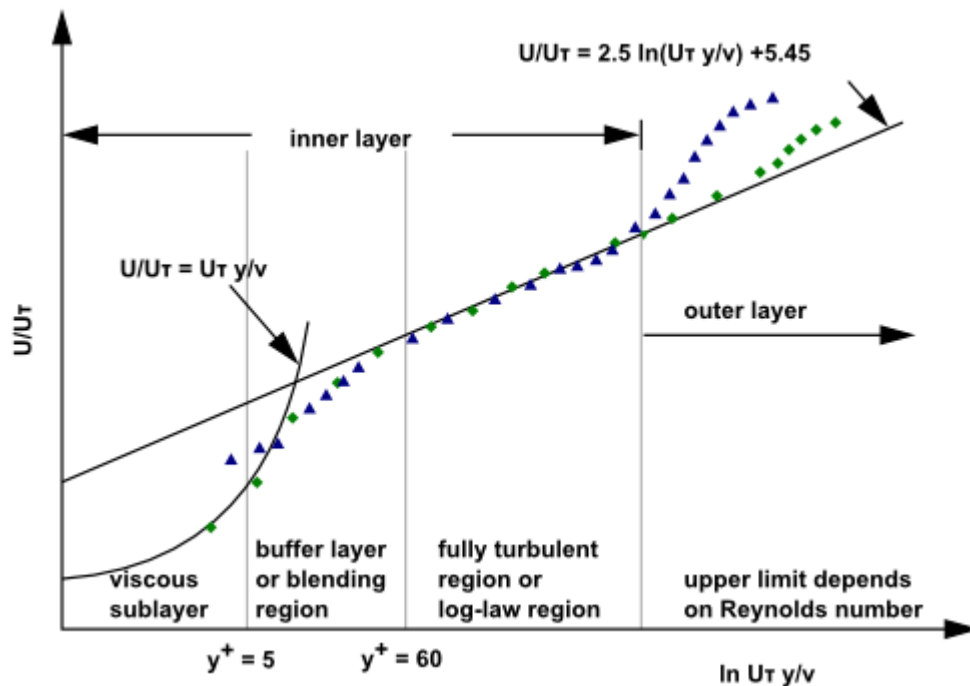

Figure 9. Turbulent sub-layers

This problem is possible to solve by using turbulent models which are more accurate in describing fluid flow in boundary layer or by using wall functions. More accurate turbulent models are rarely used because of problems with modeling of universal turbulent model and because of they are heavier on computational resources. Wall functions are developed by defining physics of fluid flow close to solid surface. Boundary layer can be separated in two characteristics sub-layers. Outer layer which is described by turbulent models and inner layer which is not possible to describe by turbulent models. In inner layer it is possible to define three more sub-layers in which different fluid flow occurs:

- Viscous sub-layer
- Buffer sub-layer
- Log-low sub-layer

Viscous sub-layer is closest to the surface and it can be assumed that has laminar flow in it. With that said viscous sub-layer molecular viscosity has vital role in transport of mass, momentum and energy. In this sub-layer turbulent viscosity is neglected and velocity profile is linear. It can be described by equation of conservation of momentum with neglecting terms of low impact like convection, pressure gradient and change of tangential component of velocity in tangential direction:

$$\mu \Delta v = \frac{\partial}{\partial n}\left(\mu \frac{\partial v}{\partial n}\right) = \frac{\partial \tau}{\partial n} = 0 \tag{11}$$

Where τ is tangential stress, μ molecular viscosity coefficient and n normal vector of solid surface. Form equation above in viscous sub-layer tangential stress is constant in direction of solid surface normal and it is equal to stress on surface.

By dimensionless terms velocity in viscous sub-layer is described by:

$$u^+ = y^+ \tag{12}$$

Where

$$u^+ = \frac{v}{v_t} \tag{13}$$

is dimensionless velocity,

$$y^+ = \frac{\rho v_t n}{\mu} \tag{14}$$

is dimensionless distance form solid surface, v_t tangential component of velocity.

Viscous sub-layer is up to height of $y^+ = 5$.

Buffer sub-layer is above viscous sub-layer. In buffer sub-layer molecular viscosity and turbulent viscosity have similar values. Moving away from viscous sub-layer influence of molecular viscosity is decreasing and turbulent viscosity is increasing. Buffer sub-layer extends form height of $y^+ = 5$ to $y^+ = 30$.

Above $y^+ = 30$ we have fully turbulent region or log-law sub-layer. In this sub-layer turbulent viscosity is dominant compared to molecular viscosity. High values of Reynolds number are present in this sub-layer so turbulent viscosity is calculated with modified turbulent model. Equation that describes that change is:

$$u = \frac{1}{\kappa}\sqrt{\frac{\tau_\omega}{\rho}}\,lny + C \tag{15}$$

Where κ is von Karman constant which value is $\kappa = 0.4187$, τ_ω tangential stress in viscous sub-layer, C integration constant. Dimensionless for of equation above is:

$$u^+ = \frac{1}{\kappa}lny^+B = \frac{1}{\kappa}ln(Ey^+) \tag{16}$$

Where B and E are constants of integration determined experimentally and value of E is: $E = 9.739$.

For good quality of velocity profile close to wall certain rules of domain discretization need to be followed. Some computing models which calculate fluid flow close to wall requires very dense discretization of domain in regions close to walls. There are two types of computing models: Wall models and Wall functions.

Wall models has certain requirements for accurate computations like, cell center of first cell along wall need to be on height of $y^+ = 1$. This is needed to correctly calculate velocity in all layers and sub-layers of boundary layer according to defined equations.

Wall functions have less demanding requirements for accurate calculations. Cell center of first cell along wall need to be on height of $y^+ = 30$ because wall functions approximates velocities in viscous and buffer sub-layer with empirical equations and solves log-low sublayer with defined equations.

Challenge that arrives with both models is generating good quality mesh which will allow correct calculation of values in boundary layer.

2.5. Conjugate Heat Transfer

For many simulation of real world engineering problems the prediction of heat transfer properties is as important if as important as fluid flow prediction. In this kind of engineering problems interest is on how heat moves through both fluid and solid. Conjugate heat transfer corresponds with the combination of heat transfer in solids and heat transfer in fluids. In solids, conduction often dominates whereas in fluids, convection usually dominates. Conjugate heat transfer is observed in many situations and it is important in many engineering problems. Gas turbines are typical engineering product with lot of conjugate heat transfer challenges. Interaction of hot gases, cold air and solid material of which gas turbine is built represents typical conjugate heat problem.

Heat Transfer in a Solid

In almost all cases heat transfer in solids is done only due to conduction. Conduction is described by Fourier's law defining the conductive heat flux q, proportional to the temperature gradient:

$$q = -k\nabla T \tag{17}$$

For a time-dependent problem, the temperature field in an immobile solid verifies the following form of the heat equation:

$$\rho C_p \frac{\partial T}{\partial t} = \nabla \cdot (k\nabla T) + Q \tag{18}$$

Heat Transfer in a Fluid

Heat transfer in fluid is very different from heat transfer in solid, because of the fluid motion. There are three contributions to the heat equation. First is the transport of fluid implies energy transport too, which appears in the heat equation as the convective contribution. Depending on the thermal properties on the fluid and on the flow regime, either the convective or the conductive heat transfer can dominate. Second is the viscous effect of the fluid flow that produces fluid heating. This term is often neglected. And third, as soon as a fluid density is temperature-dependent, a pressure work term contributes to the heat equation. This accounts for the well-known effect that for example compressing air produces heat. Accounting for these contributions, in addition to conduction, results in the following transient heat equation for the temperature field in a fluid: [8]

$$\rho C_p \frac{\partial T}{\partial t} + \rho C_p u \cdot \nabla T = \alpha_p \text{T} \left(\frac{\partial p_A}{\partial t} + u \cdot \nabla p_A \right) + \tau : \text{S} + \nabla \cdot (k\nabla T) + Q \tag{19}$$

3. Numerical method

3.1. Discretization of equations

Domain of fluid flow is commonly discretized by final volume method. Domain discretized by final volume method is divided in to N small volumes which are called control volumes (cells). Number, shape, size and distribution of cells depend on a problem of analysis.

Control volume in inertial coordinate system is volume that is stationary or it moves in constant speed and through that volume fluid flows. Boundaries of control volume are control surfaces and points in edges of control surface are called nodes.

In geometric center of control volume flow properties are calculated (velocity, pressure, temperature, etc.) by flow equations (Navier-Stokes equations). In numerical calculations values are known only in points of domain (centers of control volumes, center of control surfaces or in nodes). For flow equations it is required to discretize mathematical operators so that it is possible to calculate with already known values.

3.1.1. Coupled Algorithm

ANSYS Fluent provides three segregated types of algorithms: SIMPLE, SIMPLEC and PISO. These schemes are referred to as the pressure-based segregated algorithm. Steady-state calculations will generally use SIMPLE or SIMPLEC, while PISO is recommended for transient calculations. PISO may also be useful for steady-state and transient calculations on highly skewed meshes. In ANSYS Fluent, using the Coupled algorithm enables full pressure-velocity coupling, hence it is referred to as the pressure-based coupled algorithm.

For both cases belt and hula seal pressure-based coupled algorithm was used. Pressure-based coupled solver offers some advantages over the pressure-based segregated algorithm. The pressure-based coupled algorithm obtains a more robust and efficient single phase implementation for steady-state flows, with superior performance compared to the segregated solution schemes.

The pressure-based segregated algorithm solves the momentum equation and pressure correction equations separately. This semi-implicit solution method results in slow convergence. The coupled algorithm solves the momentum and pressure-based continuity equations together. The full implicit coupling is achieved through an implicit discretization of

pressure gradient terms in momentum equations, and an implicit discretization of the face mass flux, including the Rhie-Chow pressure dissipation term. [12]

In momentum equations the pressure gradient for component k is of the form:

$$\sum_f p_f A_k = -\sum_j a^{u_k p} P_j \tag{20}$$

where $a^{u_k p}$ is the coefficient derived from the Gauss divergence theorem and coefficients of the pressure interpolation schemes. Finally, for any i-th cell, the discretized form of momentum equation for component u_k is defined as

$$\sum_j a_{ij}^{u_k u_k} u_{kj} + \sum_j a_{ij}^{u_k p} P_j = b_i^{u_k} \tag{21}$$

In the continuity equation the balance of fluxes is replaced used the flux expression resulting in discretized form

$$\sum_k \sum_j a_{ij}^{p u_k} u_{kj} + \sum_j a_{ij}^{pp} P_j = b_i^p \tag{22}$$

As a result, the overall system of equations after being transformed to the $\delta -$ form is presented as:

$$\sum_j [A]_{ij} \vec{X}_j = \vec{B}_i \tag{23}$$

3.2.   Discretization of domain

Cells (control volumes) can be divided by shape, typical cells are:

- 2D
  - Structured control volume

    2D prism – quadrilateral ("quad")

  - Unstructured control volume
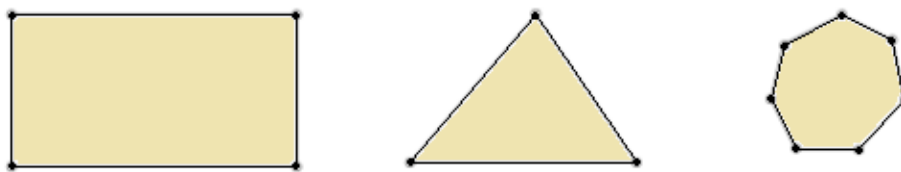
    Triangle ("tri")

    Polygon

Figure 10. 2D cells: Quad, Tri, Polygon

- 3D
  - Structured control volume

    Hexahedron ("Hex")

  - Unstructured control volume

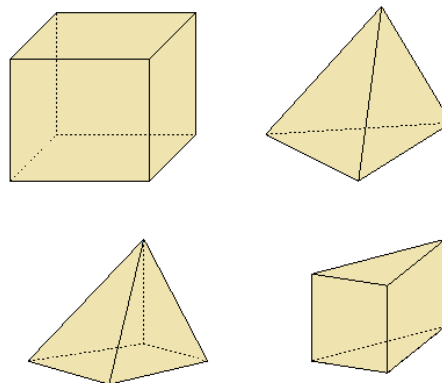   Tetrahedron ("Tet")

    Pyramid
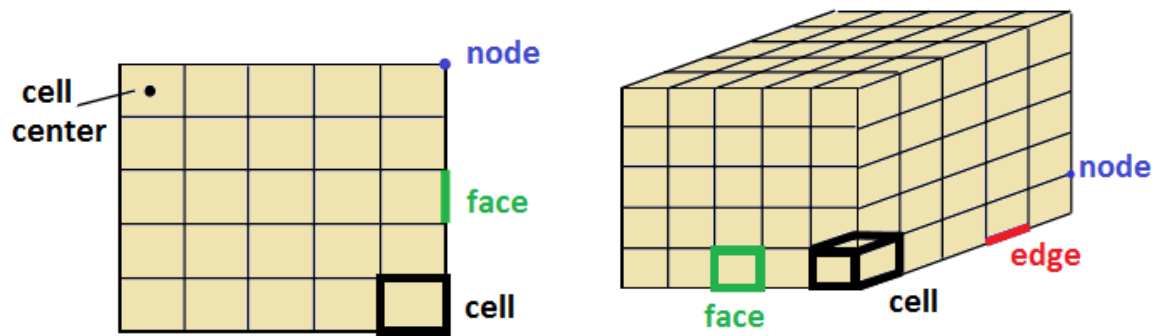
    Prism

    Polyhedral

Figure 11. 3d cells: Hex, Tet, Pyramid, Prizm

Figure 12. Discretization of 2d and 3d domain

Table 1.   Mesh nomenclature

Cell	control volume into which domain is broken up
Node	grid point
Cell center	center of a cell
Edge	Boundary of a face
Face	boundary of a cell
Zone	group of nodes, faces and cells: Wall boundary zone, Fluid cell zone
Domain	group of node, face and cell zones

Hexahedral type of cells usually gives best quality of discretization (mesh). The density of the mesh is important and requires sufficiently high order to capture all the flow features. Mesh density should not be so high to capture unnecessary details of the fluid flow. When there is a wall present in a domain, the mesh adjacent to the wall need to be fine enough to resolve the boundary layer flow. For boundary layer usually it is better to generate quad, hex or prism cells over triangles, tetrahedrons and pyramids. Quad and hex cells can be stretched where the flow is fully developed and one-dimensional.

It would be best to have as smallest number of cells as possible to shorten number of equations and with that shorten computing time. On the other hand cells need to be small enough so they don't generate error that will have big impact on result. For assessing size of cells through domain it is vital to understand and predict flow in domain.

Smallest cells should be generated near surface like walls on which no-slip condition is setup. Because of no-slip condition on the wall high gradients of velocity are present.

Mesh quality can be determined by: Rate of convergence, Solution accuracy, CPU time required and Independence of grid results. For rate of convergence, better mesh quality gives faster convergence of solution. With mesh quality too low solution may not converge due to certain phenomenon like boundary layer in fluid flow which will not be solved because of poor mesh quality. Solution accuracy depends on mesh quality if mesh is not sufficiently refined then the accuracy of solution is limited. For CPU time required to get solution on highly refined mesh will cost more time than coarse mesh. The key is to find balance between enough mesh refinement to account all important fluid behavior in domain but also coarse enough to get solution in reasonable time. Result independent grid means that more refinement of that grid will not change simulation results. As long as result of simulation is changing due to increasing of mesh refinement, mesh isn't result independent.

But mesh quality is hard to judge on requirements listed above before running simulation. Therefore some easier methods to determine mesh quality are developed.

Mesh quality or the suitability of mesh can be determined by skewness, smoothness and aspect ratio. Skewness determines how close to ideal cell actual cell is.

There are two methods for measuring skewness: one based on the equilateral volume (for tetrahedral cells) and one based on the deviation from a normalized equilateral angle. (for pyramids, prisms and hexes)

$$Skewness = \frac{Optima\ Cell\ Size - Cell\ size}{Optimal\ Cell\ size} \tag{24}$$

$$Equiangular\ Skew = max\left[\frac{\theta_{max} - \theta_e}{180 - \theta_e}, \frac{\theta_e - \theta_{min}}{\theta_e}\right] \tag{25}$$

Where: θ_{max} is the largest angle in a face or cell, θ_{min} is the smallest angle in a face or cell and θ_e is the angle for equiangular face or cell i.e. 60 for a triangle and 90 for a square. A skewness of 0 is the best possible one and a skewness of one is bad. For Hex and quad cells, skewness should not be above 0.85 to get accurate solution. [7]
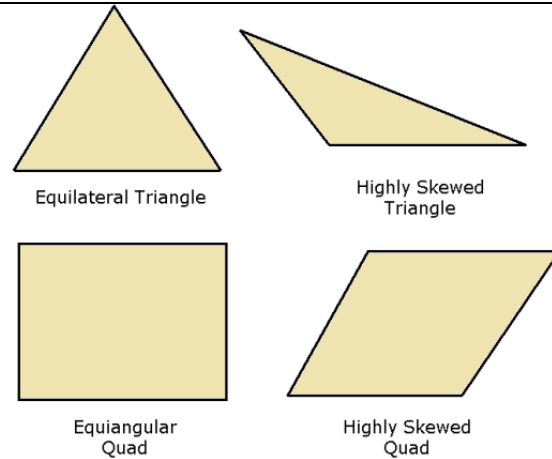
Figure 13. Skewness mesh quality

Smoothness or size change corresponds to smooth change in size. Size change is the ratio of volume of a cell in the geometry to the volume of each neighboring cell. Sudden jump in the cell size can result in bad solution results at nearby nodes.
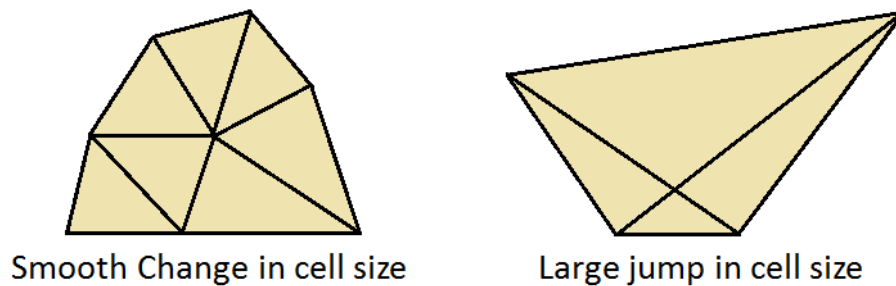

Figure 14. Change in size mesh quality

Aspect ratio is the ratio of longest edge to shortest edge of cell. It is defined differently for each element type. Aspect ratio should be equal to 1 for best results. Having a large aspect ratio can result in an interpolation error.
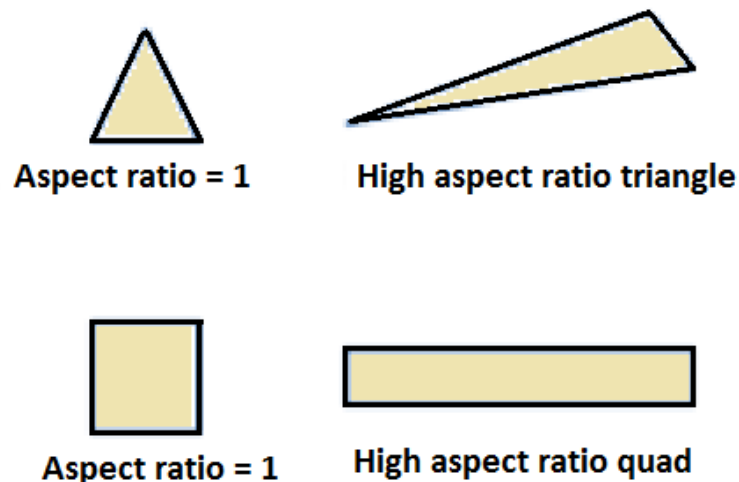
Figure 15. Aspect ratio mesh quality

4. Numerical Analysis of Interface Seal

In this chapter CFD-process for Hula seal performance analysis is describe. First geometry manipulation and modeling of geometry for Hula seal have been done. After model preparation mesh was generated for fluid and solid domain. When meshing process is done Fluent case is created and setup. Used boundary conditions and fluid properties will be presented as well as turbulence modeling choice. Same processes will be done for Belt seal so comparison between those two seals can be presented. Boundary conditions and material properties for belt and hula seal case are exactly the same, main difference is geometry of seal and mesh around it.

4.1. 3D – Modeling

For CFD analysis of hula seal performance three geometry models are needed to create domain for fluid flow: Hula seal or belt seal model, hot gas casing model and combustion inner liner model. Hot gas casing and combustion inner liner models are creating domain for fluid flow also interface between these two parts is sealed by Belt or Hula seal. Hot gas casing and combustion inner liner whole models have been acquired. Some geometry simplification and repair was performed on these models in preparation for CFD analysis. Also belt seal model have been acquired. Hula seal model was not acquired and it needed to be created. Creation of hula seal model will be performed in CATIA and rest of geometry manipulation will be done in ANSYS programs like Design Modeler and SpaceClaim. As analysis of Hula seal will be done by comparison with old design, first domain for old geometry with belt seal need to be setup.

4.1.1. Belt seal

3D models for hot gas casing, combustion inner liner and seal belt was obtained in form of parts. These three parts need to be assembled and prepared for CFD analysis. But first geometry cleaning and repair was done to remove some non-important part on the models. Process of assembly consisted of orienting models in same direction, defining contact surface between parts and defining clearance between parts. Preparation and 3d geometry manipulation was performed in Ansys SpaceClaim. Geometry that was not important for fluid flow was removed also some fillets and chamfers were removed. As CFD analysis will be done for rotational periodic sub-model, whole model that was made by assembly needed to be sliced to form rotational periodic sub-model. Sliced periodic part of belt seal model that will

be used in CFD analysis is highlighted. From that rotational periodic sub-model negative geometry was created to represent fluid domain.
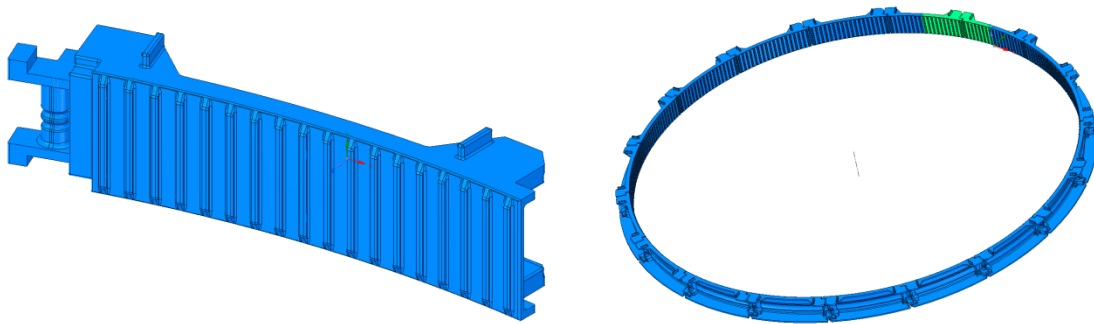

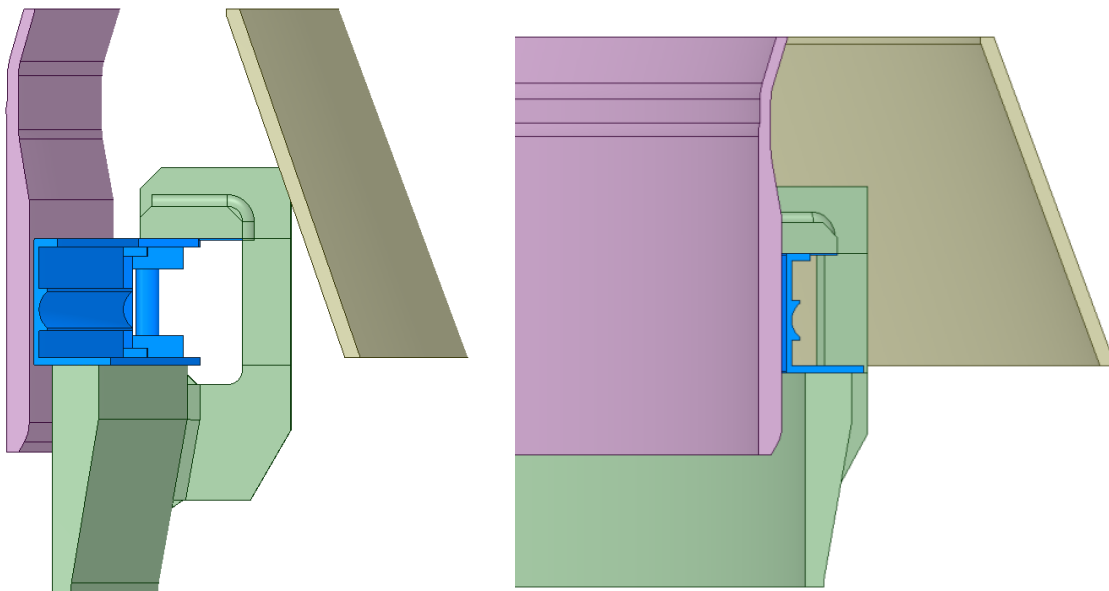**Figure 16. Belt seal 3d model one segment on left and whole belt on right side of figure**

Figure 17. Assembly model of belt seal hot gas casing and combustion inner liner

4.1.2. Belt seal model simplification

First mesh generation was done on whole model of belt seal that can be seen on left hand side of Figure 16. Because of complexity back side of belt seal model produced very high number of cells in a mesh also due to lot of small and curved surface mesh quality in that area was low. This low quality mesh with very high cell number made convergence of solution very slow and difficult also providing some non-physical behavior of fluid. Because of that, geometry of belt seal model simplification was done. Results of simplification can be seen on right hand side of Figure 16. Mesh that was generated on new geometry had better average quality of mesh and cell count was almost halved.
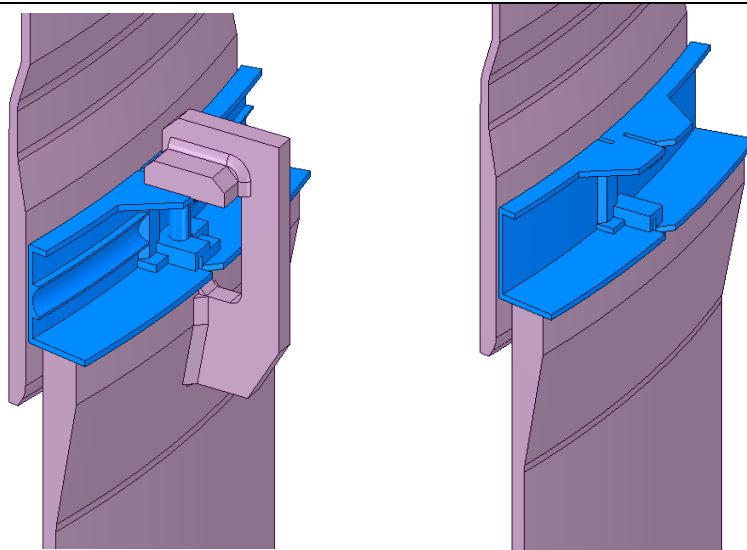
Figure 18. Belt seal 3d model simplification

4.1.3.   Hula seal

Hula seal 3d model could not be obtained so it needed to be made. To design 3D model of hula seal recommendations from commonly owned U.S. Pat. No. 6,334,310 were used. 3D model of hula seal was design in CATIA. After designing hula seal in CATIA, assembly of hot gas casing, combustion inner liner and hula seal was done in ANSYS SpaceClaim. Like for the belt seal similar job needed to be done for hula seal. As CFD analysis will be done for rotational periodic sub-model, whole model that was made by assembly needed to be sliced to form rotational periodic sub-model. On Figure 19 sliced periodic part of hula seal model that will be used in CFD analysis is highlighted. From that rotational periodic sub-model negative geometry was created to represent fluid domain. [1]
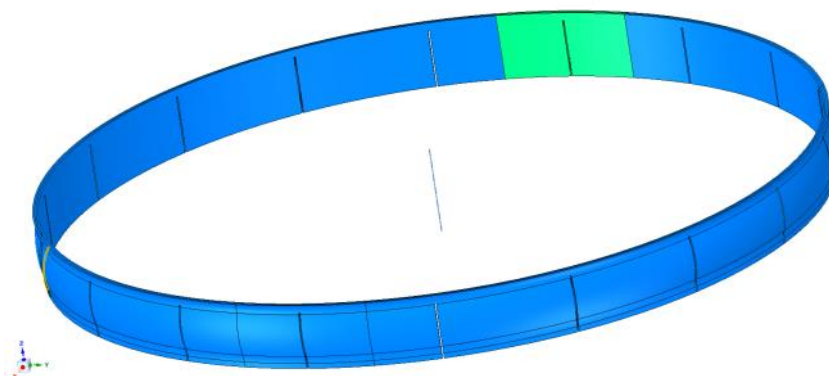

Figure 19. Hula Seal 3d model

Not only that geometry for hula seal has been created but also hot gas casing needed to be modified to fit hula seal. Holders of belt seal were removed from hot gas casing and it was extended to fit hula seal in space between combustion inner liner and hot gas casing.
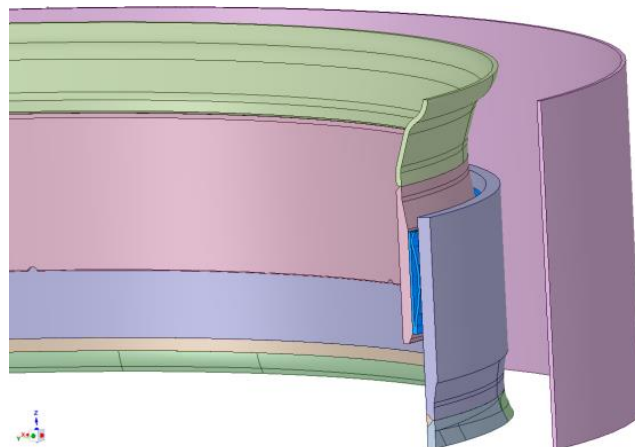
Figure 20. Assembly model of hula seal hot gas casing and combustion inner liner

4.1.4. Periodicity of interface sealing

Periodic flow occurs when the physical geometry of interest and the expected pattern of the flow/thermal solution have a periodically repeating nature. Main reason for using periodic sub-model instead of full models is reducing the size of mesh and with that shortening time need for generating meshing itself as well as shortening time of computing the solution.

Interface between hot gas casing and combustion inner liner with interface seal can be separated in periodic parts. Number of periodic parts is defied by number of segments of belt seal, and for hula seal number of periodic parts is defined by number of gaps on hula seal. Both belt and hula seal have 18 periodic parts.

For belt seal case half of two belt segments were used to create periodic sub-model because of leakage that is happening at connection between two segments. Leakage that is happening between two segments is important for downstream flow characteristics and temperature field of both fluid and solid domain. For hula case choice where to slice domain to create periodic sub-model was much easier due to much simpler geometry of hula seal compared to belt seal. Figure 21 shows place where belt and hula were sliced to form periodic sub-model.
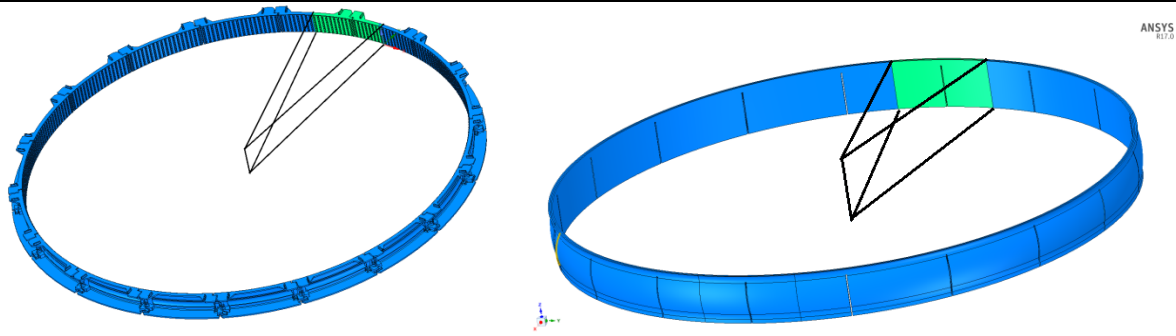
Figure 21. Periodic slice of belt and hula seal

The air and gas channels were built around the seal, as show in Figure 22. These channels are small parts of actual hot gas and air paths. On the side walls of these channels the periodic conditions were applied.
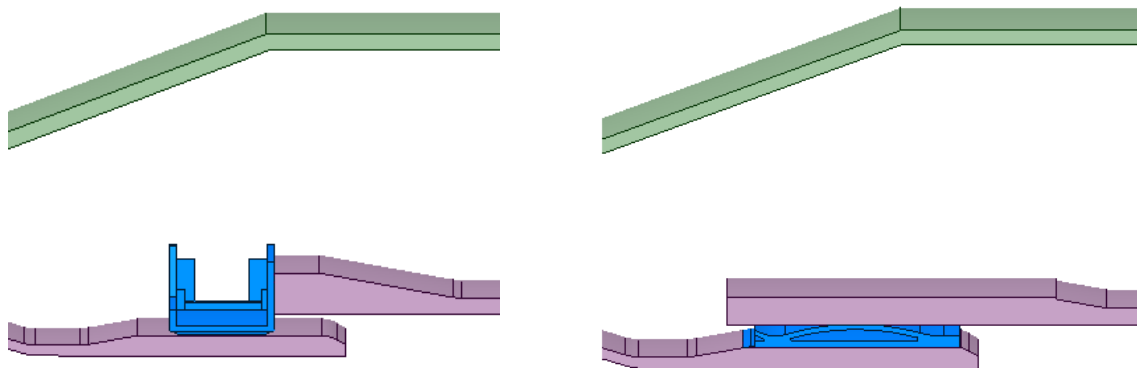

Figure 22. Periodically sliced assembly of belt and hula seal

4.1.5.   Creating domain of fluid flow

The CAD model of belt and hula seal segments joint is shown in Figure 22. The model contains end parts of two seal segments and their joint. It also includes neighboring parts of combustion inner liner and hot gas casing. In the model used for calculations both the hot gas casing and combustion inner liner were extended by cylindrical surface in order to shift outlet of calculation domain away from the area of interest. Same process of extending model with cylindrical surface was done for air and gas outlets. Extension of hot gas casing and combustion inner liner can be observed on Figure 23 and Figure 24. After extensions of domain for solid part of domain was done, negative domain was created to represent fluid domain which can be seen on Figure 25 and Figure 26.
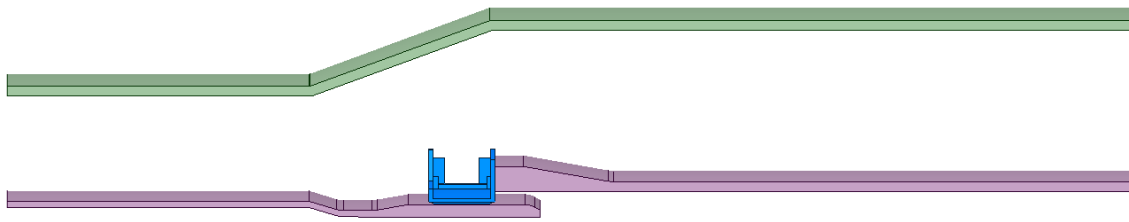
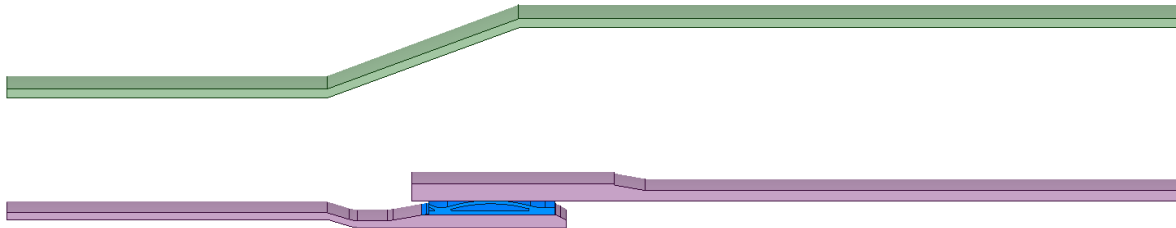**Figure 23. Assembly of belt seal domain extended by cylindrical surfaces**

Figure 24. Assembly of hula seal domain extended by cylindrical surfaces

Because this is conjugate heat transfers problem discretization of domain or mesh need to be generated for fluid and for solid. Solid mesh will be generated inside assembly parts like seals, hot gas casing and combustion inner liner. For fluid negative geometry form assembled part need to be created and then mesh for fluid domain is generated in that negative geometry. On Figure 25 and Figure 26 solid domain is colored by magenta and fluid domain which is created from solid parts is colored blue. On this domains fluid and solid mesh will be generated respectively. Surface mesh on contact between fluid and solid domain will be exactly the same for fluid and sold or we can say it will be conformal.

Figure 25 and Figure 26 shows how domains of belt and hula seal looks like after all geometry manipulations. These domains consist of fluid and solid. Fluid part of domain is colored blue on figures and solid part of domain is colored magenta. Fluid and solid parts of domain are separated by surfaces and these surfaces also belong to both fluid and solid. On this geometry of fluid and solid from Figure 25 and Figure 26 mesh will be generated.

The lower boundaries of gas flow were sliced to reduce size of generated mesh because no important fluid flow is happening there. Boundary condition use at the bottom of domains is symmetry plane. The no-slip adiabatic conditions are applied on all solid walls.
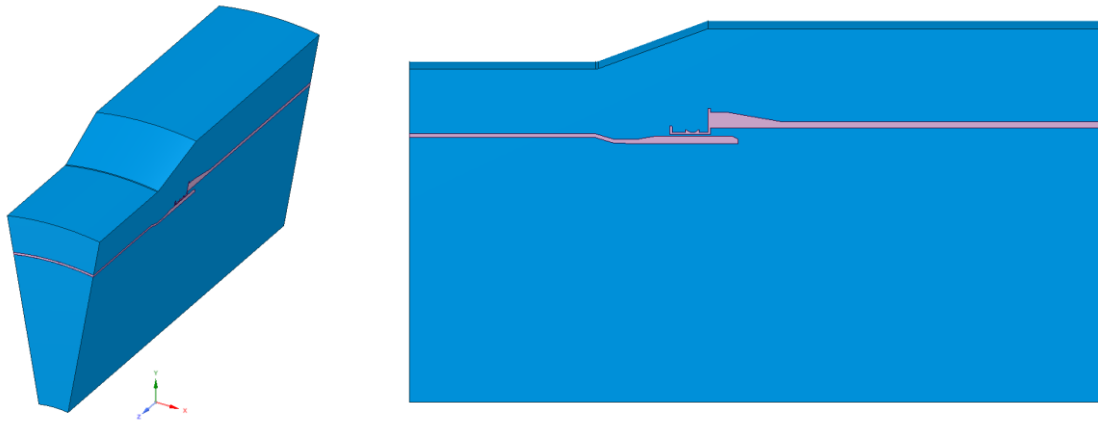
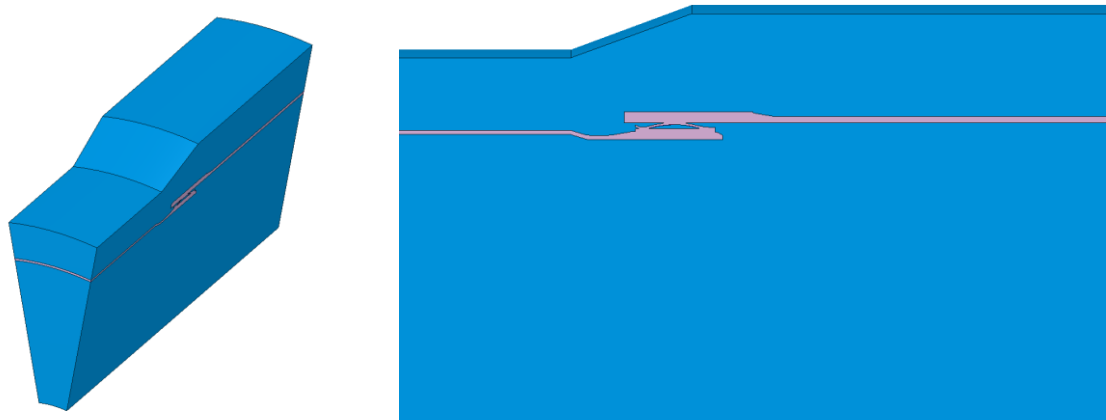**Figure 25. Belt computational domain, fluid – blue, solid - magenta**

Figure 26. Hula computational domain, fluid – blue, solid - magenta

4.2.   Mesh generation

Mesh generation for Hula and Belt seal case, flow and solid part of domain was done in Ansys ICEM. Geometry prepared in Ansys SpaceClaim was imported in Ansys ICEM where bad surfaces were repaired and some geometry preparation for meshing was done. After repairing geometry volume mesh was generated. First fluid part of domain was populated with tetrahedral cells than layers of prism cells were generated on walls of domain. After fluid domain was done mesh for solid part of domain was generated. Fluid and solid part of domain share surfaces that are connecting them. Mesh on connecting surfaces is exactly the same for fluid and solid part of domain to avoid errors of interpolation which is used when non-conformal surfaces are used for connection. Similarly is done for surface on which periodic boundary condition will be applied. It is important for sub-models like in this thesis to

generate exactly same surface mesh on the periodic surface to avoid errors of interpolation that is used if surface mesh isn't conformal. More refined mesh (smaller cells) is used in parts of fluid domain where complex fluid flow is anticipated. Those are areas around and close to seal itself, especially in gaps of seals where fluid is leaked from cold air side to hot side of domain. Whole domain and mesh of belt and hula seal can be seen on Figure 27.
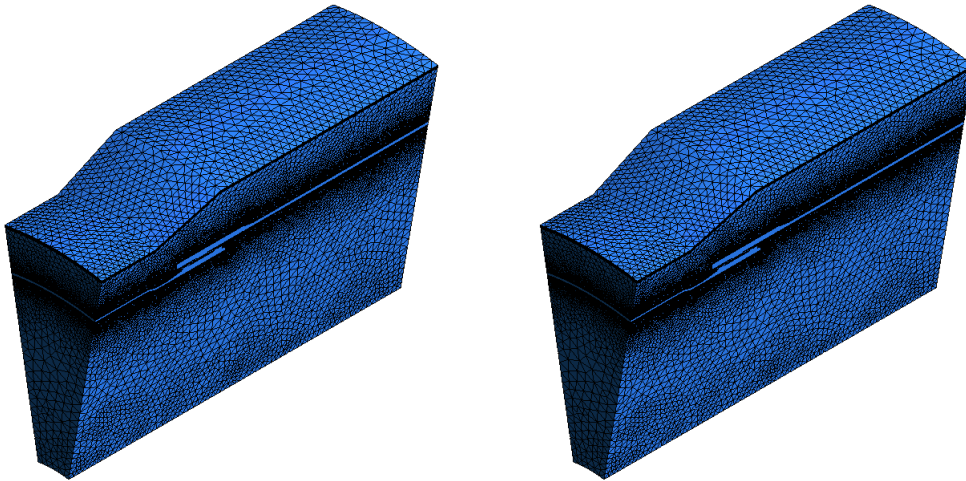
Figure 27. Mesh of whole belt (left) and hula (right) seal domain
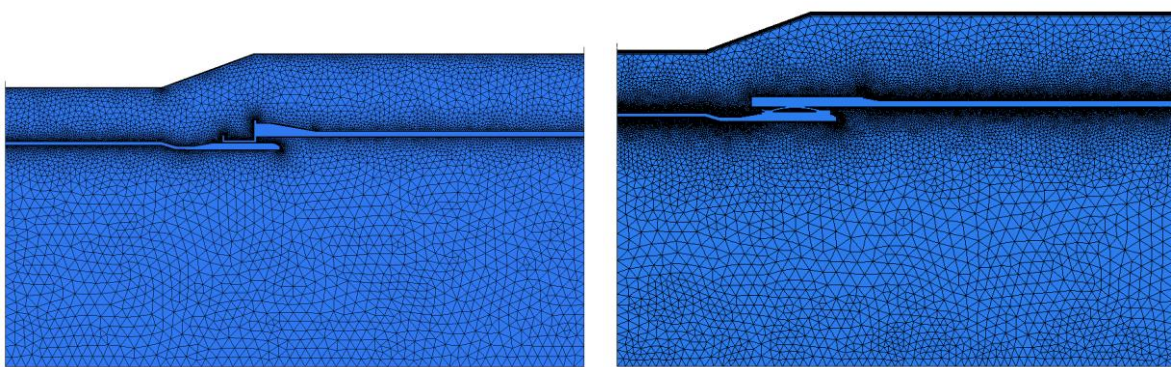
Figure 28. Fluid domain discretization on periodic surface of belt (left) and hula (right) seal

Whole fluid mesh of belt and hula seal domain can be seen on Figure 28. After domain was populated with tetrahedral cells, mesh check in ANSYS ICEM was preform to observe mesh quality and repair worst cells. Mesh smoothing was done to increase quality of generated mesh. When tetrahedral mesh reached good enough quality via mesh smoothing in ANSYS ICEM, prism layers were generated one by one to get proper mesh near walls, in order to allow proper calculation of flow in boundary layer. Mesh of fluid domain around seals can be seen on Figure 29. When fluid mesh was generated similar process was done for solid part of

domain except near wall mesh doesn't need so much refinement as in fluid. Figure 30 presents mesh of solid part of domain for both belt and hula seal.
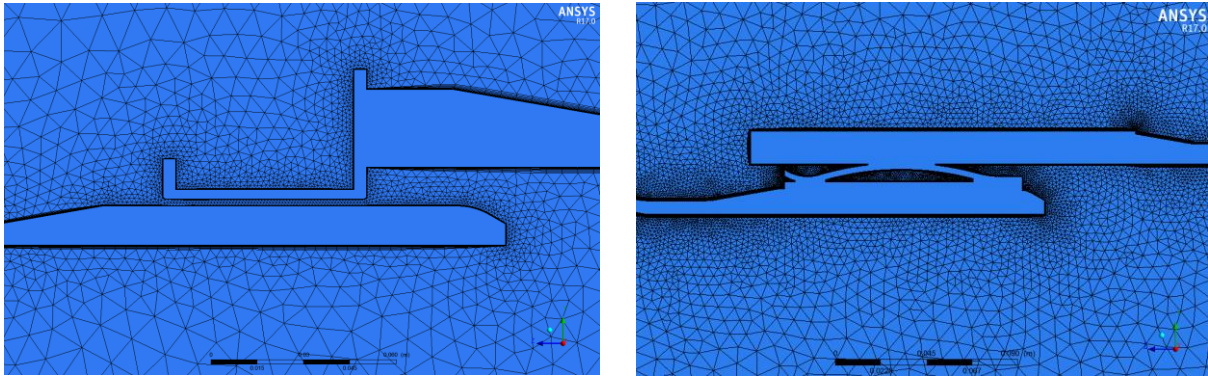

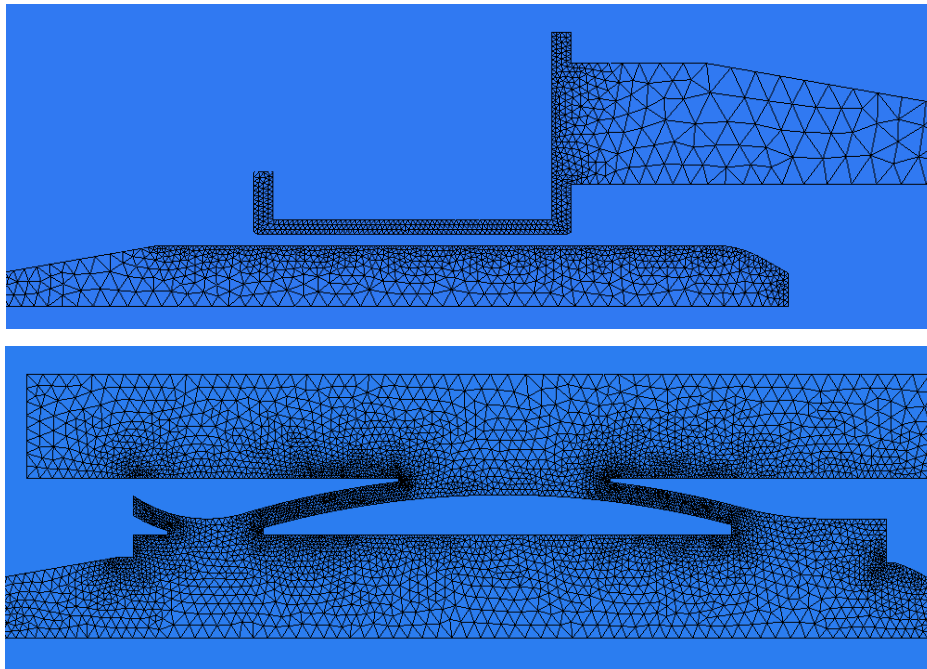**Figure 29. Fluid domain discretization around belt and hula seal**

Figure 30. Solid domain discretization of a belt (top) and hula (bottom) seal

Domain of flow for both belt seal and hula seal is axisymmetric divided in 18 equal parts. Generated meshes are unstructured. Most complex part of geometries is seal itself. Velocity of fluid flow should be maximal in gaps of seal. Along all the walls on fluid side of domain prism cells are extruded to form boundary layer. Height of first prism cells in boundary layer is defined by requirements of y+ for turbulence model, in our case k-epsilon with enhanced wall treatment. $y+$ at the wall-adjacent cell should be on the order of $y+ \leq 1$. However, a higher $y+$ is acceptable as long as it is well inside the viscous sub-layer ($y+ \leq 4\ to\ 5$). To

satisfy $y+ \leq 1$ values height of first prism need to be around $1e - 06$. Prisms that are creating boundary layer on walls can be seen on Figure 31. Prism growth is set for 1.2 multiplications for each next prism. 25 prism layers were generated to form boundary layer.
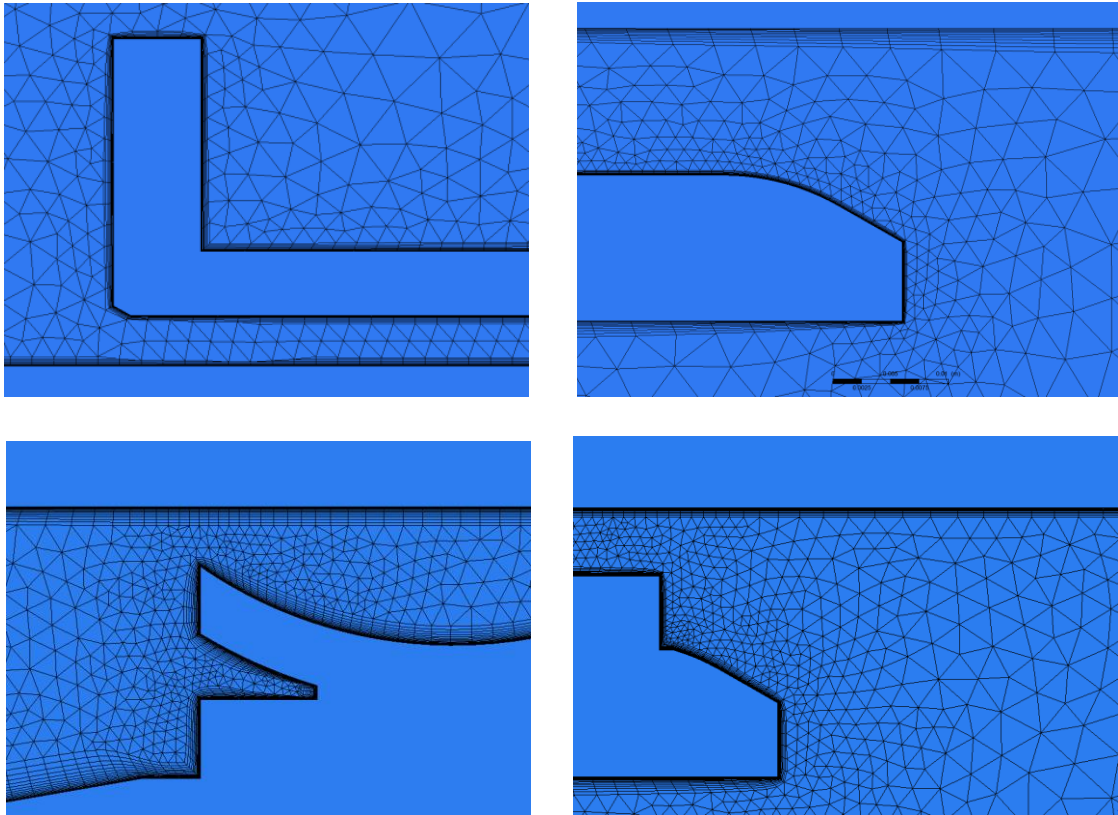

Figure 31. Mesh around seal

Y+ is non-dimensional wall distance for a wall-bounded flow. It can be defined as following:

$$y^+ = \frac{u_* \cdot y}{\nu} \tag{26}$$

where u_* is the friction velocity at the nearest wall, y is the distance to the nearest wall and ν is the local kinematic viscosity of the fluid.

Mesh in solid part of domain need to be generated to calculate interaction of heat flow between fluid and solid. Also heat transfer through solids: hot gas casing, combustion inner liner and seals were calculated.

Table 2.   Mesh information's

	Belt seal	**Hula seal**
Number of Cells:	19356156	16754132
Fluid mesh:	11949172	9976471
Solid mesh:	7406984	6777661

Check command in fluent verifies the validity of the mesh. The check provides volume statistics, mesh topology and periodic boundary information, verification of simplex counters, and verification of node position with reference to the x axis for axisymmetric cases.

The mesh checking capability in ANSYS Fluent examines various aspects of the mesh, including mesh topology, periodic boundaries, simplex counters, and node position with respect to the x axis, and provides a mesh check report with details about the mesh.

The mesh check examines the topological information, beginning with the number of faces and nodes per cell. A tetrahedral cell (3D) should have 4 nodes. Next, the face handedness and face node order for each zone is checked. The zone should contain all right-handed faces, and all faces should have the correct node order. The last topological verification is checking the element-type consistency.

The quality of the mesh plays a significant role in the accuracy and stability of the numerical solution. Regardless of mesh used in domain, checking the quality of mesh is essential. Orthogonal quality is important indicator of mesh quality that ANSYS Fluent allows you to check. 12

4.3.   Simulation setup

Hula and Belt seal case will be simulated with same boundary conditions and same case setup in order to compare performances for this two seals. Only difference between this two cases pre-computing is geometry and of course mesh. Meshes for both domains were generated with same settings so the meshes of belt and hula seal domain are very similar. Sub-model are also almost the same because of same periodic rotational conditions. Both sub-model are 1/18 of whole assembly model.

Domains in which fluid flow is calculated are tri-dimensional rotational periodic sub-model. Solver type used for simulation for seal of interface between hot gas casing and combustion liner is Pressure-Based Navier-Stokes solution algorithm. Steady state flow will be solved.

For turbulence model realizable $k - \epsilon$ model with enhanced wall treatment was used.

4.3.1. Materials

In ANSYS Fluent case before calculation material settings has to be defined. In our domain for belt and hula seal same materials were used. For the fluids in domain (air and gas) air fluid material was used with properties provided form ANSYS Fluent material database. Density of air is chosen to be described as ideal gas. By choosing ideal gas for density of fluid material compressible flow was defined. Describing air as ideal gas means that density of air depends on temperature and pressure.

For solid material steel was chosen from ANSYS Fluent material database as a basic material.

Table 3.   Thermal properties of steel

Description	*Label*	*Value*	*Unit*
Density	ρ	8030	kg/m^3
The specific heat	c$_p$	502.48	J/(kgK)
Thermal conductivity	λ	16.27	W/(mK)

Table 4.   Thermal properties of air

Description	*Label*	*Value*	*Unit*
The specific heat for a constant pressure	c$_p$	1,006	kJ/(kgK)
Thermal conductivity of fluid	λ_F	0,0242	W/(mK)
Dynamic viscosity	μ	1,7894x10^{-5}	Pas

4.3.2.   Boundary conditions

Surfaces that are boundary of domain are divided into:

- Inlet

- Outlet

- Wall

- Symmetry

- Periodic

- Coupled Wall

On our domain we have two inlets and two outlets. Inlets are defined with pressure-inlet boundary condition and outlets with pressure-outlet boundary condition. Temperatures and pressures used in this thesis are assumptions of conditions in real gas turbine. Values of pressure for inlets and outlets that are used in this thesis are given in Table 5 also temperatures of fluid are defined on inlets. Temperature set on outlet boundary conditions are only if backflow occurs and real values will be calculated via simulation.

For pressure inlet and pressure outlet following boundary condition were applied:

Table 5.   Inlet and Outlet boundary conditions

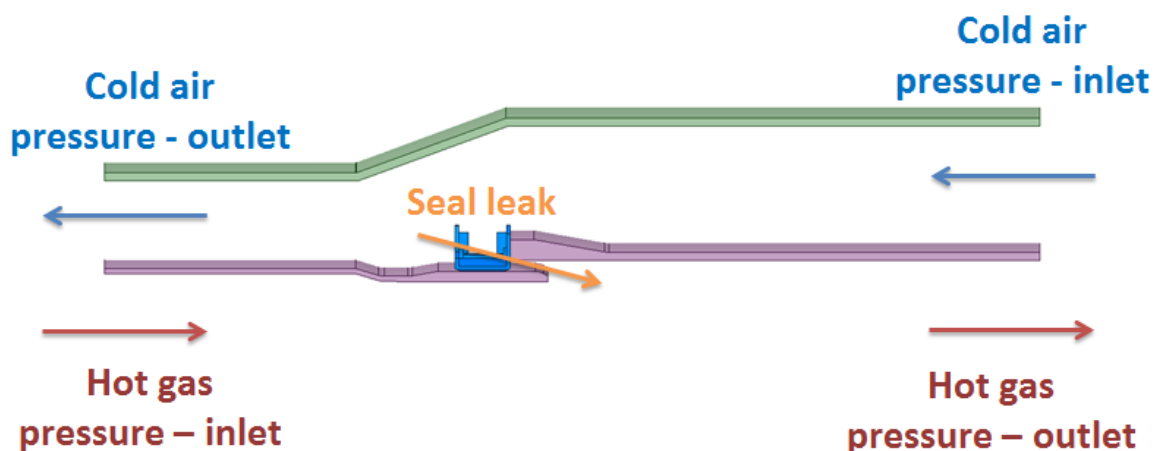| *Surface*	*Boundary condition*	*Pressure kpa*	*Temperature K*
Air Inlet	Pressure-inlet	1260	650
Air Outlet	Pressure-outlet	1240	600
Gas Inlet	Pressure-inlet	1215	1400
Gas Outlet	Pressure-outlet	1200	1350

Figure 32. Fluid flow in domain

On surface on top of domain we have adiabatic wall thermal boundary condition with no slip boundary condition. Surface of seals, hot gas casing and combustion inner liner are separating fluid form solid part of domain. On those surface thermal coupled wall boundary condition is set also on side of fluid no slip boundary condition is set. On surface on bottom of domain symmetry boundary condition is applied. Surfaces on sides of domain are equal in size and shape and have periodic boundary condition applied on them. All boundary condition applied in these two cases can be observed on Table 6 and surface on which they are applied on can be seen of Figure 33.

Table 6.   **Boundary conditions**

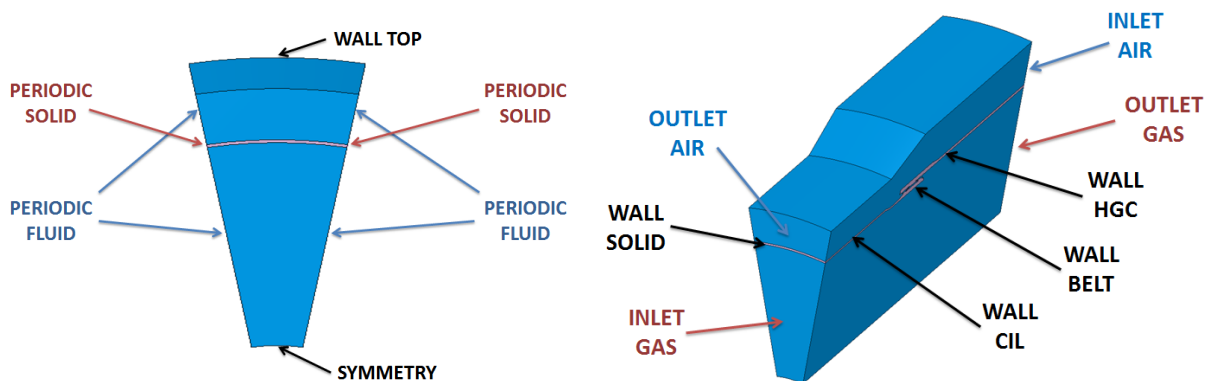| *Surface*	*Boundary condition*
Wall Top	Adiabatic wall
Wall HGC	Coupled wall
Wall CIL	Coupled wall
Wall Belt	Coupled wall
Periodic Fluid	Periodic
Periodic Solid	Periodic
Wall Solid	Adiabatic wall
Wall Bot	Symmetry

Figure 33. Boundary conditions applied on surfaces of domain

All walls in domain have no-slip boundary condition. Periodic surfaces are set in pairs with periodic boundary condition. Surface mesh on periodic pairs is exactly the same, meshes of solid and fluid are conformal. Periodic boundary condition virtually connects mesh, cells of surface pair in a way that cells which have faces on periodic surface share common control surface. Mapping of surface periodic pair is done by pairing nodes between two surfaces and

calculating, interpolating coefficients. With help of this coefficient's interpolations are done between paired nodes and because of that it is not necessary to have exactly same mesh at both of paired surfaces. But for minimizing interpolation error exactly same mesh was created on paired surfaces with periodic boundary condition. On bottom side of domain symmetry boundary condition was set. Between fluid and solid meshes are conformal surface, exactly the same mesh for both fluid and solid in all contact regions.

4.3.3. Initialization of solution

Before starting CFD simulation of interface seal, initial guess of the solution flow must be provided. In ANSYS Fluent two methods for initializing the solution which will initialize the entire flow field (all cells):

- Standard initialization
- Hybrid initialization

For our cases hybrid initialization was used because it provided better convergences at start of calculation then standard initialization.

Hybrid initialization is a collection of recipes and boundary interpolation methods. It solves Laplace's equation to determine the velocity and pressure fields. All other variables will be automatically patched based on domain average values or a particular interpolation recipe.

5. Results of numerical analysis

In presented results emphasis will be on comparing two seals, hula and belt seal. All results in figures and numbers were exported form ANSYS Fluent or ANSYS CFD post tool.

5.1. Pressure Fields

Fields of static pressure were generated for belt and hula seal domain for easier comparison of fluid flow in those two domains. Higher pressure can be seen on cold air side of domain than pressure on hot gas side of domain. That difference in pressure generate stream of cold air from cold side to hot side through gaps in belt and hula seal. Same pressure boundary conditions were set for both cases so distribution of pressure in domain of belt seal and hula seal will be similar. Some differences in pressure field can be observed around seals. Pressure fields can be observed on cross section of seals fluid domain on figures: Figure 34 and Figure 35. On left hand side of figures field of pressure for whole domain can be observed and on right side is close-up of seals.
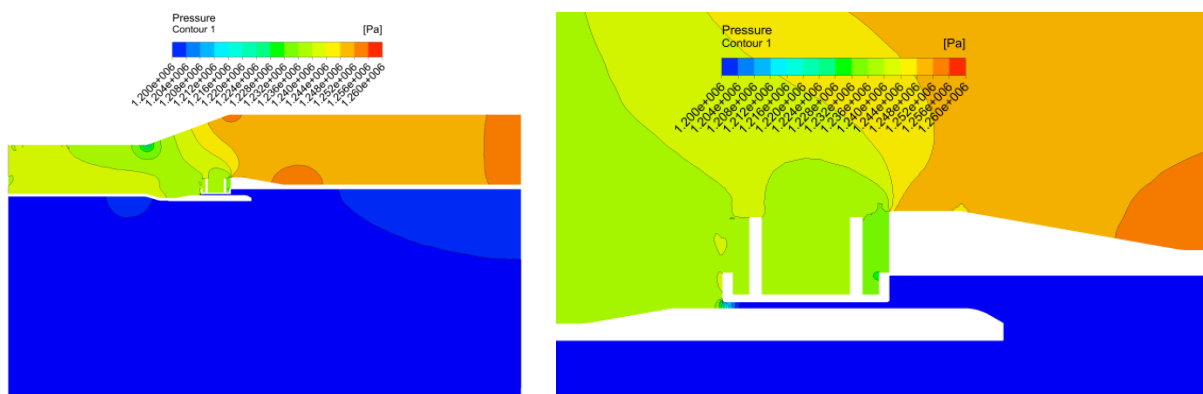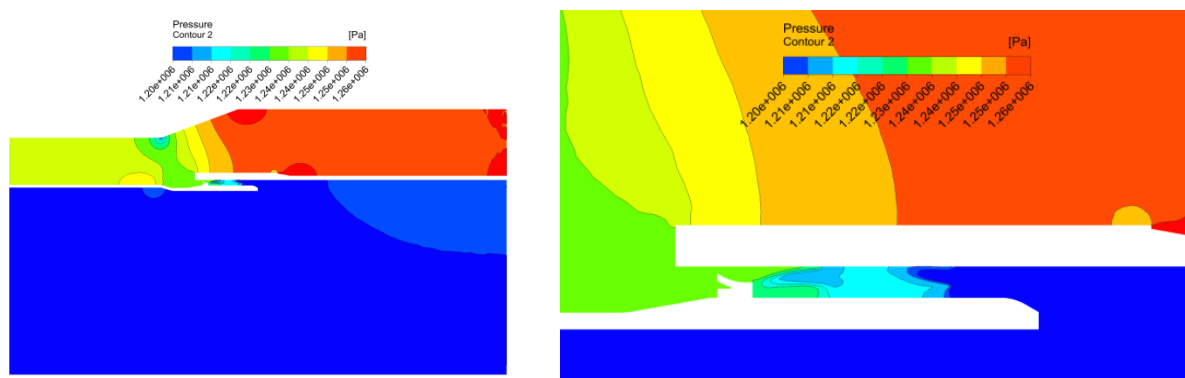
Figure 34. Belt seal, static pressure field

Figure 35. Hula seal, static pressure field

5.2. Velocity Fields

Figures of velocity field were generated for belt and hula seal domain for easier comparison of fluid flow in those two domains. That difference in pressure generate stream of cold air from cold side to hot side through gaps in belt and hula seal. From Figure 36 and Figure 37 we can see that fluid flow has highest values of value in gaps of seals. On left hand side of figures field of pressure for whole domain can be observed and on right side is close-up of seals. Maximum velocity is around 110 m/s in gaps of belt and hula seal.
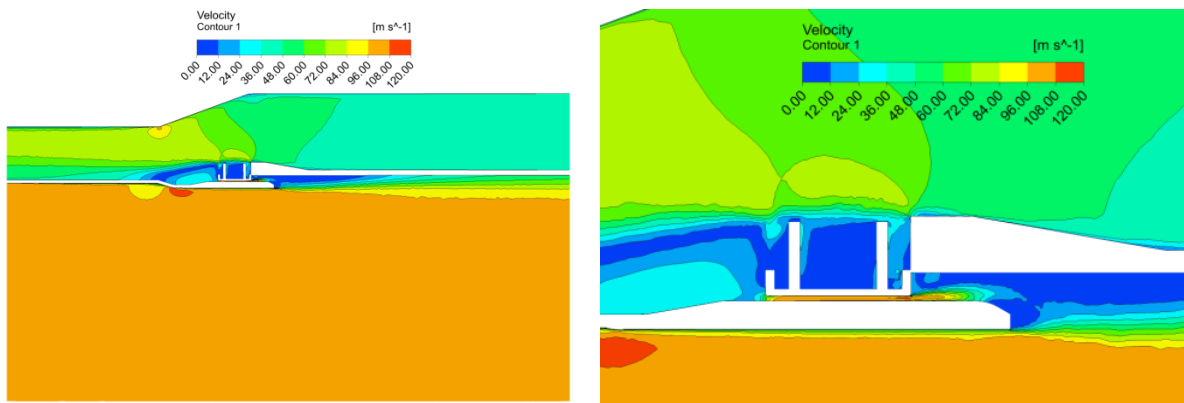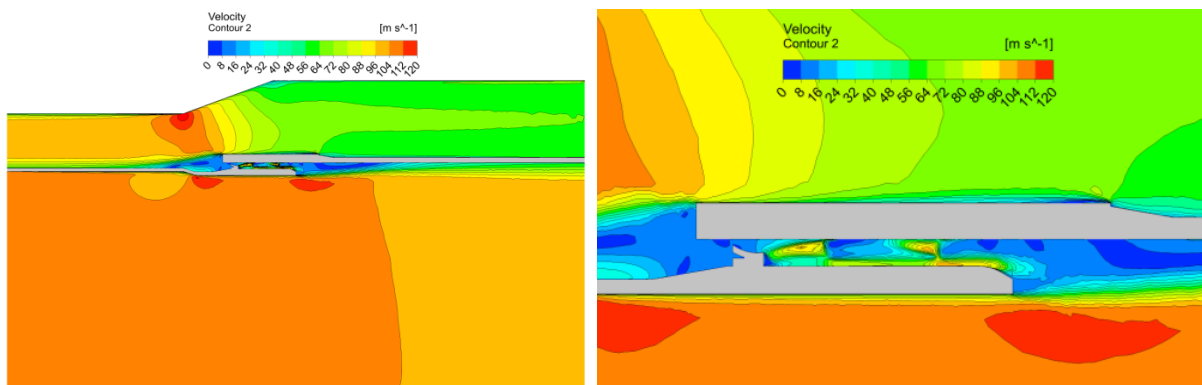

Figure 36. Velocity field of belt seal domain

Figure 37. Velocity field of Hula seal domain

5.3.   Temperature Field

Temperature field on cross-section of seals are presented on Figure 38 and Figure 39. Cold air from top of domain is cooling solid. Small part of cold air is leaked through gaps of seals form cold side to hot side of domain. Air that is leaked is cooling interface of hot gas casing and combustion inner liner as well as seal of that interface, belt and hula seal. After passing through gap of seal cold air is cooling hot gas casing on inside and also mixing with hot gases. These processes can be observed on figures below.
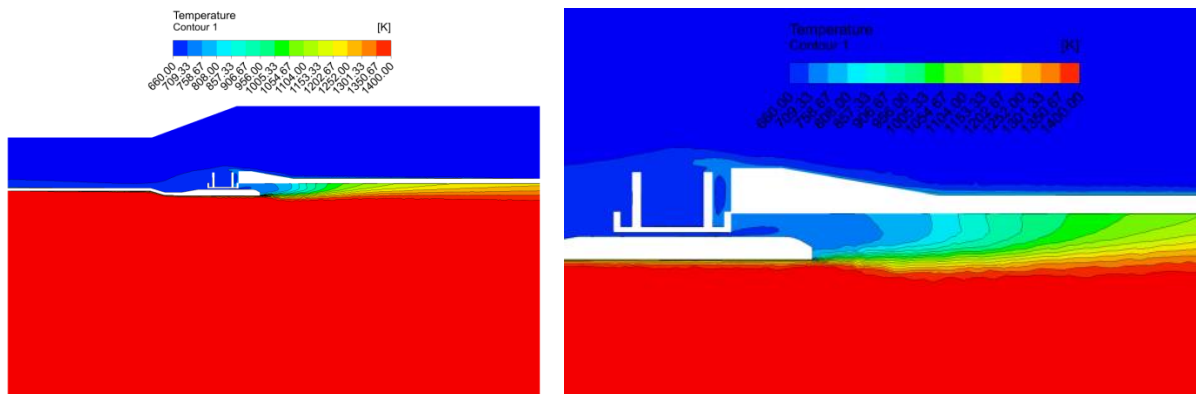

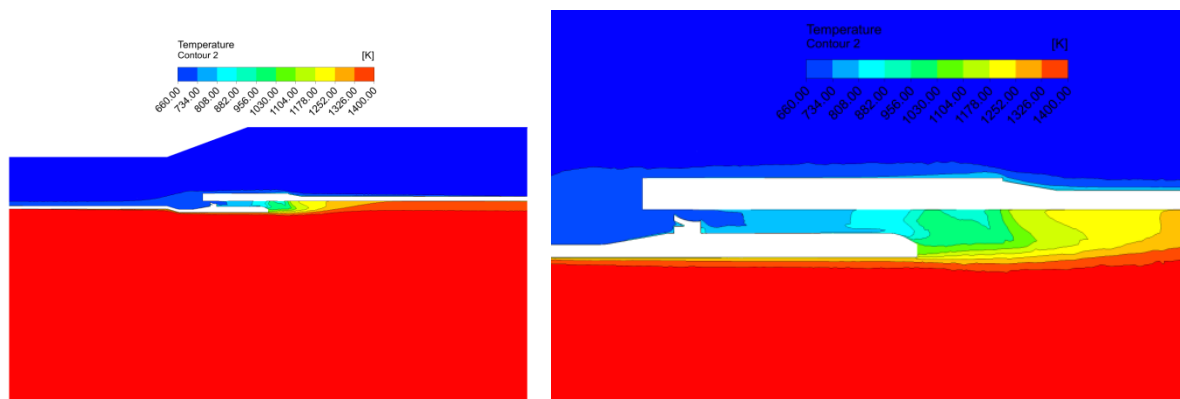**Figure 38. Belt seal temperature field**

Figure 39. Hula seal temperature field

On Figure 40 and Figure 41 temperature field on solid surfaces are given. Figures show how hot gases and cold air effects on temperature of solids in domain. From these figures temperature distribution on solid surface can be seen. Lowest temperature of solids surface are around seals because that part are cooled from more than one sides also cooing is provided via streaming of cold air through gaps in seals.
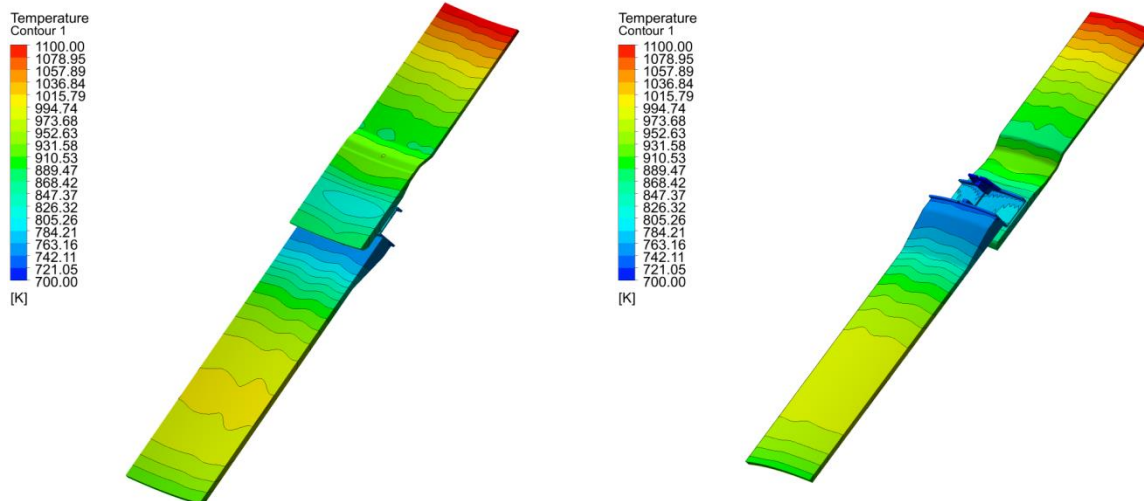

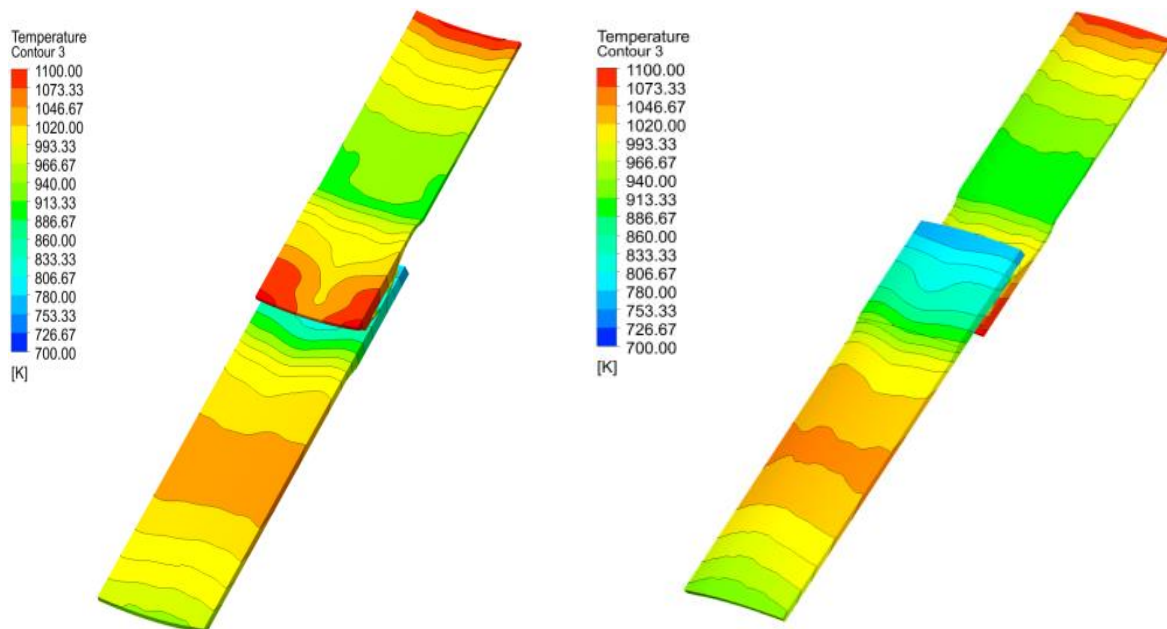**Figure 40. Temperatures on solids surfaces of belt seal case**

Figure 41. Temperatures on solids surfaces of hula seal case

On hula seal case solid temperatures on bottom of combustion inner liner are very high compared to same place on belt seal case. This is due to better distribution of cooling provided by belt seal. Also on hot gas casing side hula seal case has higher temperatures compare to belt seal case.

On Figure 42 heat transfer coefficients on surfaces of solid are presented, on the left hand side is belt seal case and on the right side is hula seal case. Heat transfer conditions are corresponding to temperatures on solid surface and to flow structure of fluid domain. On bottom part of combustion inner liner values of heat transfer coefficient are high on areas where highest temperatures are for hula seal case that can be seen on Figure 41. Similarly, solid temperatures on hot gas casing are higher for hula seal case. Accordingly heat transfer coefficients are higher on that area on hula seal case. This is direct consequence of fluid flow structure.
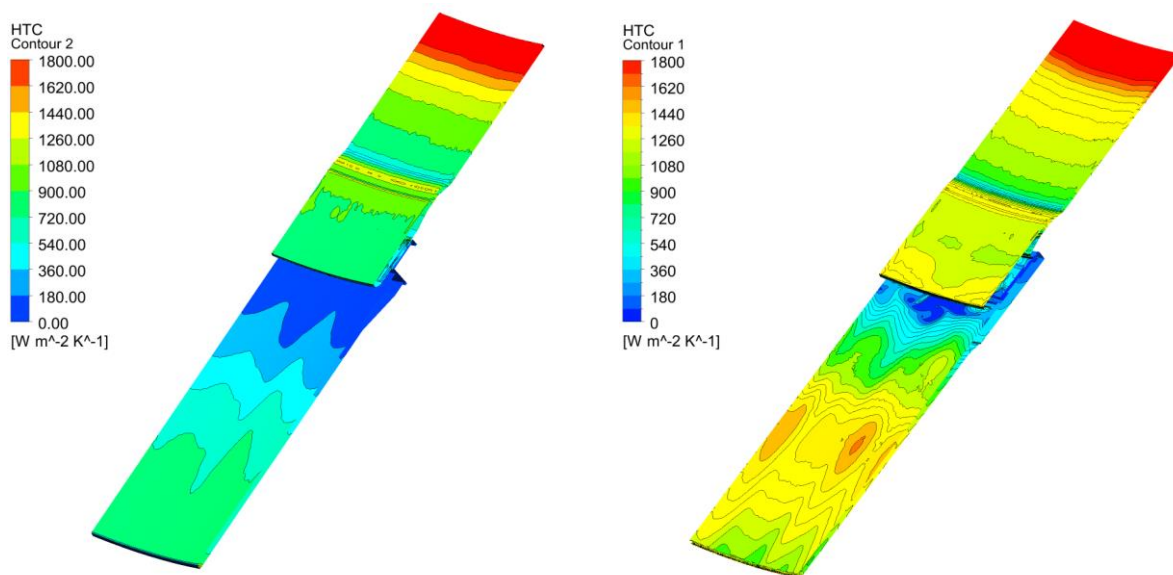

Figure 42. Heat transfer coefficients on surfaces of belt (left) and hula (right) seal case

5.4.   Flow structure

Flow structure of belt and hula seal case will be presented by streamlines. First stream of cold air colored by velocity field through gaps of seal and then interaction between cold air and hot gases. This behavior of fluid presented by streamlines affects temperatures of fluid and solid in domain. Solid wall temperatures on figures above are consequence of fluid flow explained in this chapter.

On Figure 43 and Figure 44 streamlines are colored by velocity field and they represent flow of cold air streaming through gaps of seals from cold side to hot side of domain. Cold air fluid behavior is observed, like recirculation before entering gaps of seals. Some recirculation is happening inside of hula seal as well. Also increase in velocity while cold air is streaming through gaps can be observed by different color of streamlines. After cold air exits gaps of seals it is mixing with hot gases, also some recirculation of cold air can be observed for belt seal case. Much more recirculation is observed after cold fluid exits gap of hula seal.

Gaps of belt and hula seal are different in size. Belt seal has much more gaps, but hula seal have much larger one. Result of this geometry difference can be observe in different behavior of cold air stream after exiting from seal gaps and by difference in cooling observed on figures of solid wall temperatures above.
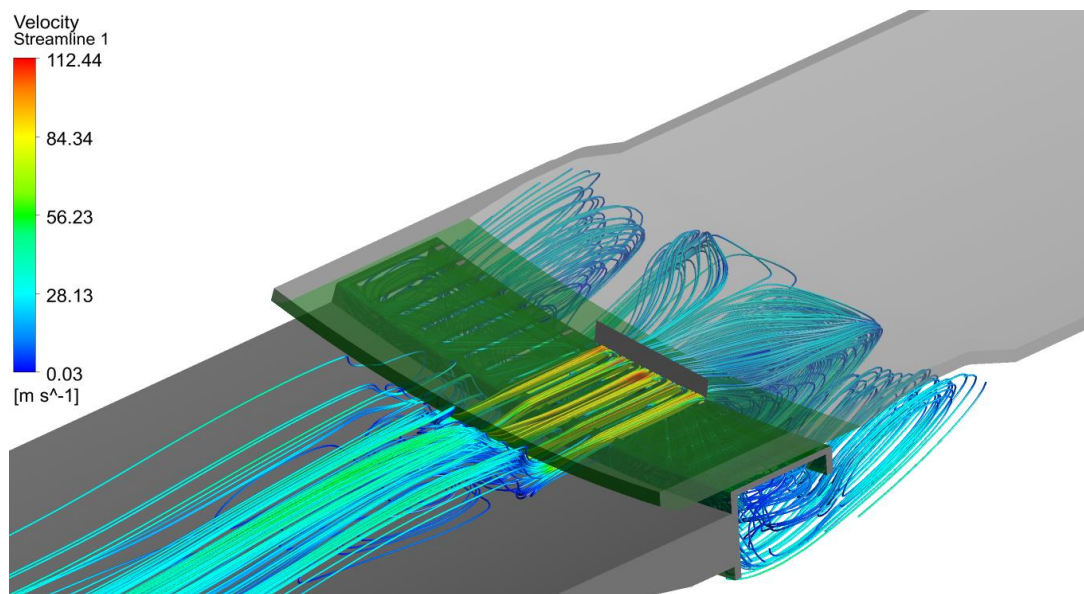

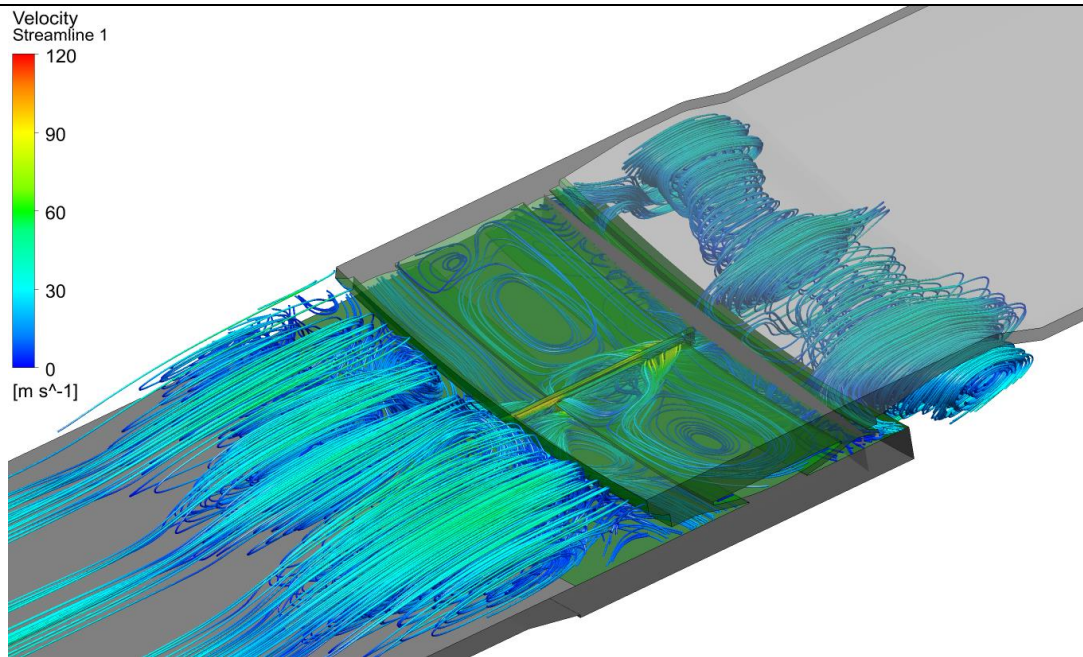**Figure 43. Streamlines of belt seal case colored by velocity**

Figure 44. Streamlines of hula seal case colored by velocity

On figures below interaction between hot gases and cold air is presented. After exiting gaps of belt seal cold air is heated and mixed with hot gases. Figure 45 shows stream lines which represents fluid flow around belt seal.
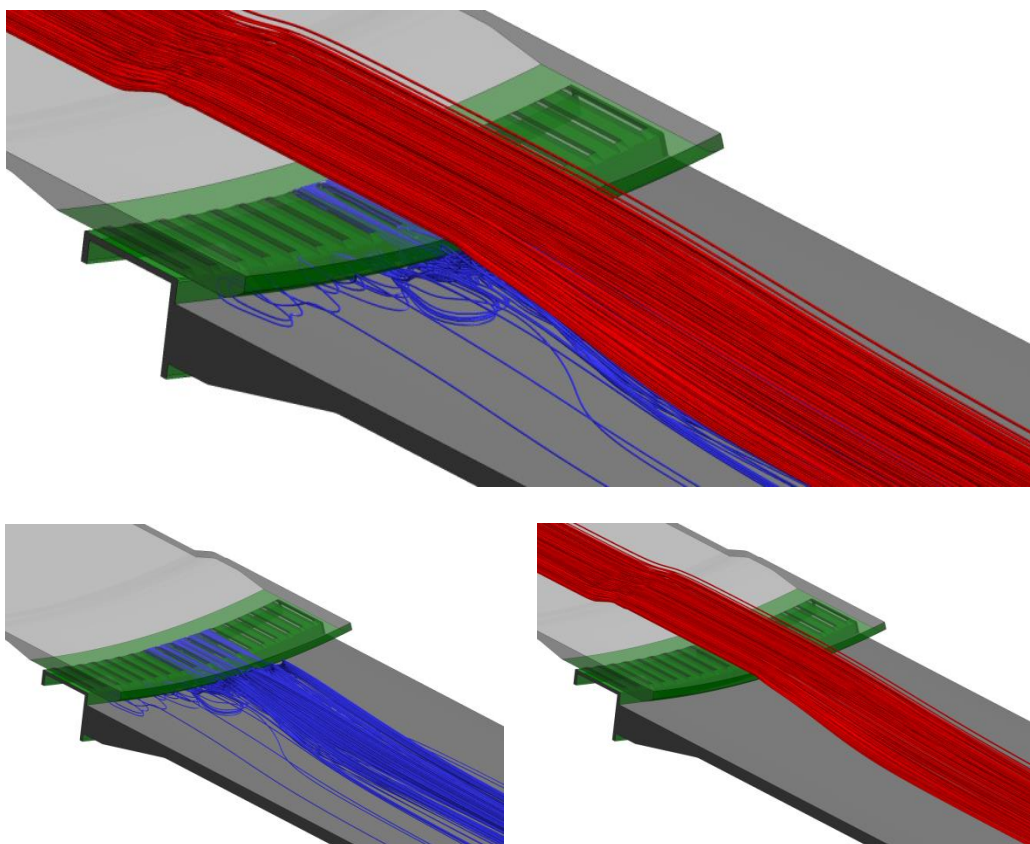

Figure 45. Belt seal streamlines, red – hot gases, blue – cold air

Red stream lines represent hot gases and blue streamlines represent cold air. As it can be seen in figures cold air is streaming through gaps of belt seal from cold air side to hot gases side of domain, that stream we call leakage. This leakage through gaps provides cooling of hot gas casing and combustion inner liner interface and seals itself that is necessary for longer lifetime of these components. After cold air exits gaps of belt seal it is heated and mixing with hot gases, also some recirculation of cold air can be observed.

Recirculation of cold air after streaming through gap of seal in hula seal case is much more visible compared to belt seal case. That recirculation is of cold gases is pulling some hot gases down toward hot gas casing and bottom part of combustion inner line. This phenomenon can be observed on Figure 46. Result of this is higher solid temperatures on bottom part of combustion inner liner and higher temperatures of hot gas casing overall for hula seal case.

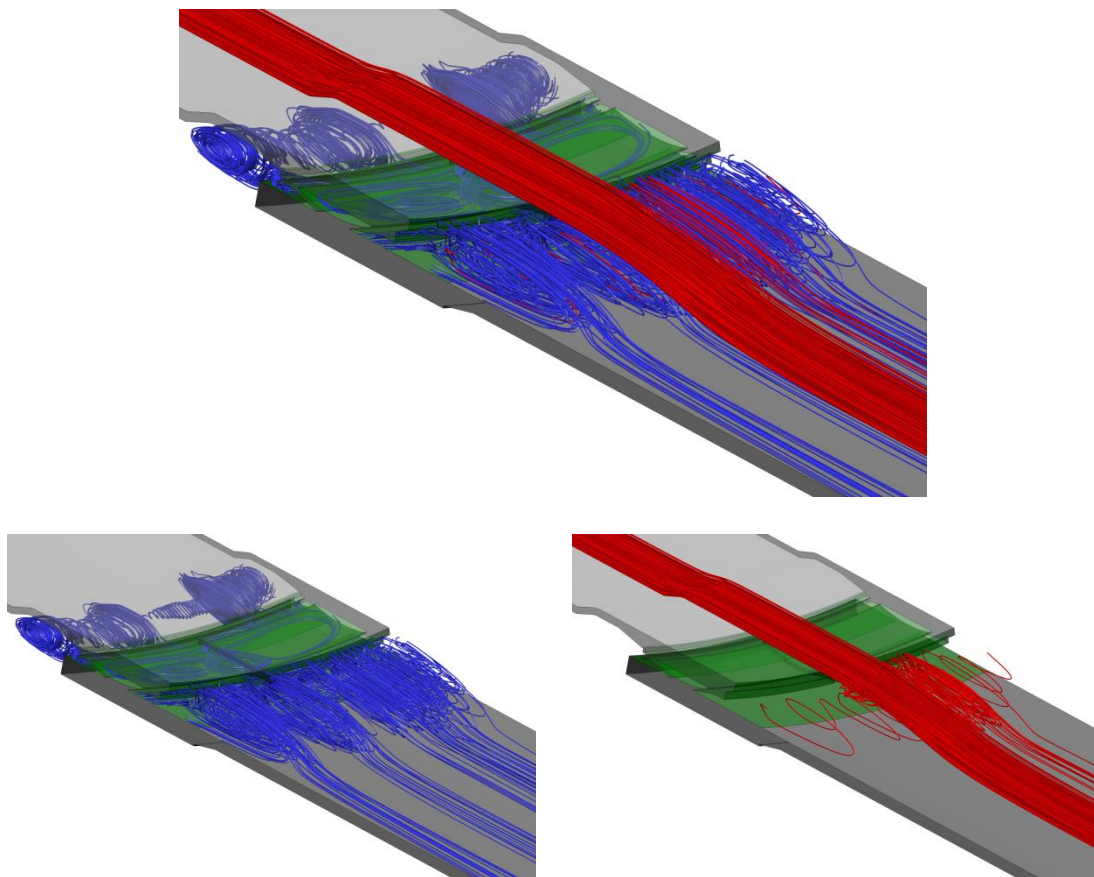This behavior can lead to hot gas ingestion and local overheating on the inner liner and hot gas casing.

Figure 46. Hula seal streamlines, red – hot gases, blue – cold air

5.5. Mass flows

Second important factor that is examined by this numerical analysis is mass flow of cold air through gaps of seal or leakage mass flow. To implement hula seal instead belt seal in gas turbine that is already working for several years on site, mass flow of cold air going to combustion chamber must remain unchanged. Which mean that seal leakage though belt seal and hula seal should be same for same working condition of gas turbine. In this thesis only one working condition of gas turbine was examined. Numerical analysis yield mass flow that can be observed on Table 7.

Table 7.   Mass flow of leakage through belt and hula seal

Mass Flow						
Sub-model				**Whole model**		
	Belt Seal	**Hula Seal**		**Belt Seal**	**Hula Seal**	
Air Inlet	15,17	14,69	kg/s	273,06	264,4	kg/s
Air Outlet	14,93	14,49	kg/s	268,74	260,8	kg/s
Gas Inlet	22,07	21,21	kg/s	397,26	381,8	kg/s
Gas Outlet	22,32	21,4	kg/s	401,76	385,2	kg/s
Seal leakage	**0,24**	**0,18**	**kg/s**	**4,32**	**3,24**	**kg/s**

From table above we can conclude that geometry changes made to fit hula seal in belt seal place changed cold air mass flow going to combustion chamber and with that hot gas mass flow was also changed. Leakage through hula seal is smaller compared to belt seal. Lowering of mass flow that is cooling this interface and seal itself provided higher solid wall temperatures.

6. Conclusion

In the last chapter results of numerical analysis of belt and hula seal performance were presented. All conclusions and observations that will be given will refer to results from chapter 5. Comparison of cooling for belt and hula case is given in form of solid surface temperatures on Figure 47. Belt seal case is on left hand side of figure and hula seal is on the right. By examining contours of temperatures on solid surface we can conclude that hula seal is not providing enough cooling compared to belt seal. Biggest differences between two cases are temperatures on bottom part of combustion inner liner. Those hot spots that are occurring on combustion inner liner would have big impact on that part lifetime. There is also difference in temperatures on hot gas casing. For hula seal case hot gas casing has high temperatures and overall look like it has worse cooling performance than compared belt seal case.
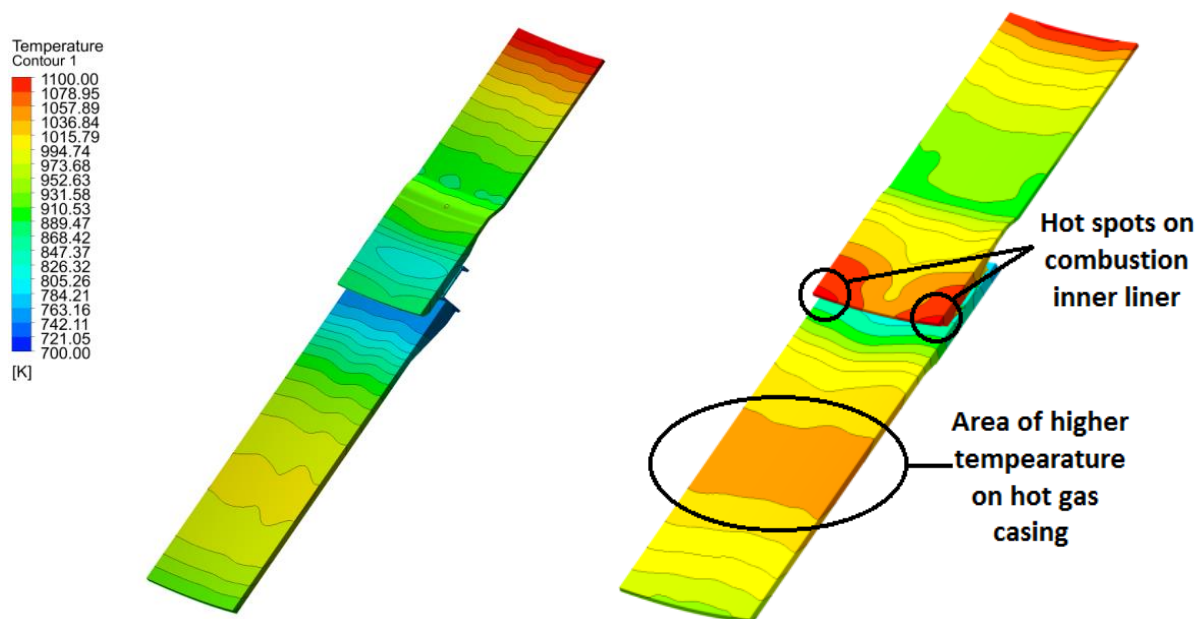

Figure 47. Comparison of temperatures on solid surface, belt seal (left), hula seal (right)

Expected benefits from the application of hula seal were: improved lifetime of the hot gas casing and inner liner, reduction of manufacturing costs and on-site assembly time. All these benefits are possible only if hula seal provides adequate cooling for interface of combustion inner liner and hot gas casing with unchanged mass flow of leak through seal gaps. Hula seal that was numerically analyzed in this thesis do not satisfies this conditions. Cooling performances of hula seal was lower compared to belt seal. Also mass flows in gas turbine combustion area were changed.

There are three reasons of poor cooling performances of hula seal. One is recirculating fluid flow of cold air after exiting gap of hula seal that pulls hot gases down to solid surface of hot gas casing. This flow structure can be observed on Figure 46. Second is reduced mass flow of leaks through gaps of hula seal compared to belt seal. Results of numerical analyses mass flows can be seen on Table 7. And third is small number of gaps on hula seal that results in hot spots on combustion inner liner. Hot spots can be seen on Figure 41 and Figure 47.

Hula seal analyzed in this thesis has only 20 gaps. To increase hula seal performance number of gaps must be increased. Increasing the number of gaps to high enough number will reduce hot spots on combustion inner liner. To maintain mass flow of cold air leakage size of every gap need to be reduced. Optimal mass flow of cold air leak that should be achieved is belt seal leak mass flow. We could consider smaller mass flow but only if cooling performances are satisfied. Increasing number of gaps and decreasing size of every gap should have positive impact on flow structure especially in area where cold air exits from seal gaps, problem of recirculation and pulling hot gases down to surface of hot gas casing should be solved or reduced.

After increasing number of gaps on hula seal numerical analysis should be conducted again with same conditions. Results should be compared to result in this analysis to see if improved performance is obtained.

References

[1]   Hula seal patent, https://www.google.com/patents/US20100300116

[2]   Versteeg, H. and Malalasekera, W.: An Introduction to Computational Fluid Dynamics, Pearson Education Limited, 2nd edition, 2007.

[3]   Z. Virag and I. Džijan, Računalna dinamika fluida – lectures, Zagreb 2015.

[4]   Belt seal patent, http://www.google.st/patents/EP2450533A1?cl=en

[5]   H. Jasak, Numerical Solution Algorithms for Compressible Flows, Zagreb, 2007

[6]   S. Patankar, Numerical Heat transfer and Fluid Flow, Tylor & Francis, 1980

[7]   "cfd-online", Online https://www.cfd-online.com/

[8]   Multyphysics cyclopedia, https://www.comsol.com/blogs/conjugate-heat-transfer/

[9]   Ching Jen Chen and Shenq-Yuh Jaw, Fundamentals of turbulence modeling, Washington, DC : Taylor & Francis, 1998.

[10] Andersson, B., Andersson, R., Håkansson, L.,Mortensen, M.,Sudiyo, R. and van Wachem, B,. Computational fluid dynamics for engineers, Cambridge: Cambridge University Press, 2012.

[11] Hot gas casing patent, https://www.google.com/patents/US4339925

[12] ANSYS FLUENT 12.0 User Guide, April 2009, www.ansys.com